APPENDIX Q

REMOTE SENSING ANALYSIS

APPENDIX Q

REMOTE SENSING ANALYSIS

TABLE OF CONTENTS

		Page
Q.1	**INTRODUCTION**	Q-1
Q.2	**REMOTE SENSING SYSTEMS AND DATA MANIPULATION**	Q-1
2.1	Satellite Systems	Q-1
2.2	Satellite Data	Q-2
2.3	Conventional Data Classification Methods	Q-3
2.4	Hardware and Software	Q-3
Q.3	**STUDY AREA AND METHODOLOGY**	Q-4
3.1	Out Line of Study Area	Q-4
3.2	Acquisition of Remote Sensing Data	Q-4
3.3	Procedure of Analysis	Q-5
3.4	Pre-Processing of Satellite Data	Q-5
Q.4	**QUALITATIVE ANALYSIS OF VOLCANIC DAMAGE**	Q-6
Q.5	**QUANTITATIVE ANALYSIS OF DAMAGE AND CHANGES**	Q-7
5.1	Damage Assessment Due to Mt. Pinatubo Eruption	Q-8
5.2	Change Analysis by Multi-Temporal Satellite Data	Q-10
5.3	Change Assessment in Watershed Basis	Q-11
Q.6	**ASSESSMENT OF VEGETATION RECOVERY**	Q-12
Q.7	**COMMENTS AND RECOMMENDATIONS**	Q-14
7.1	Accuracy of Classified Remote Sensing Data	Q-14
7.2	Recommendation for Future Works	Q-15

LIST OF TABLES

Table No.	Title	Page
Q.1	Characteristics of commonly used satellites and their sensors	Q-16
Q.2	Major fields of application of the Landsat TM spectral bands	Q-16
Q.3	Landsat Thematic Mapper Data Information	Q-17
Q.4	Daily Rainfall in Sacobia River Basin in 1991	Q-18
Q.5	Daily Rainfall in Sacobia River Basin in 1992	Q-19
Q.6	Daily Rainfall in Sacobia River Basin in 1993	Q-20

LIST OF FIGURES

Figure No.	Title	Page
Q.1	Spectral response patterns of typical land cover classes	Q-21
Q.2	General procedure of digital classification of remotely sensed data	Q-22
Q.3	Hardware and software configuration used for analysis	Q-23
Q.4	Location of the study area and the major river network	Q-24
Q.5	Pyroclastic and lahar estimates by DPWH	Q-25
Q.6	Criteria of satellite data analysis for the study	Q-26
Q.7	Natural color composite of 1990 January TM data	Q-27
Q.8	Natural color composite of 1990 July TM data	Q-27
Q.9	Natural color composite of 1992 February TM data	Q-28
Q.10	Natural color composite of 1992 November TM data	Q-28
Q.11	Natural color composite of 1993 February TM data	Q-29
Q.12	Natural color composite of 1993 December TM data	Q-29
Q.13	Natural color composite of North-West part of the study area	Q-30
Q.14	Natural color composite of North-East part of the study area	Q-31
Q.15	Natural color composite of South-East part of the study area	Q-32
Q.16	Spectral response patterns of Landsat TM data of 1992 February	Q-33
Q.17	Estimation of pyroclastic and lahar extent by 1992 February TM data	Q-34
Q.18	Comparison of 1992 February TM data estimation of damaged area with DPWH surveys	Q-35
Q.19	Spectral response patterns of Landsat TM data of 1993 February	Q-36
Q.20	Spectral response patterns of Landsat TM data of 1993 December	Q-36
Q.21	Estimation of pyroclastic and lahar extent for multitemporal TM datasets	Q-37
Q.22.1	Changes between damaged extents as observed by TM data classification	Q-38
Q.22.2	Changes between damaged extents as observed by TM data classification	Q-39
Q.23	Comparison of DPWH and TM data estimation for 1992 and 1993	Q-40
Q.24	Defined zones for detailed investigation of damage and changes	Q-41
Q.25	Estimation of NDVI changes during 1992 February to 1993 February and 1992 November to 1993 December	Q-42
Q.26	Frequency distribution of pixels with increased NDVI for defined zones for the period of 1992 February to 1993 February	Q-43
Q.27	Frequency distribution of pixels with increased NDVI for defined zones for the period of 1992 February to 1993 February	Q-44

Q.1. INTRODUCTION

Eruption of Mt. Pinatubo in 1991 produced voluminous ash fall and pyroclastic flow. Erupted materials settled on the mountain slopes were eroded with the intensive rainfall experienced during the following rainy seasons disturbing the natural and social life of most of the adjoining provinces.

The question of erosion and mudflow during monsoon seasons said to be the most devastating secondary disaster that can further complicate the situation in this region. Engineering expertise are investigating the best possible ways to reduce the damage to life and property by constructing necessary engineering structures. Detailed analysis of lahar flow, accurate information on topography and related geographical features are integrated for better designing procedures. Along with these detail investigations, it is required to study the damage of the eruption and the consequences by investigating the incident collectively. this will facilitate to gather more information on the spread of lahar flow due to rainfall, changes occur in the region within the damage area and its surrounding, possible secondary disaster due to excessive lahar deposits, comparison of changes in zone basis, etc. Satellite data is becoming advantageous in studying temporal changes as the repeated coverage of the same place on the earth is possible. Further, it is comparatively cheaper to use satellite data and there is no other source that will furnish information on a incident that have been occurred in the past.

Use of satellite data was indispensable for the Pinatubo Rehabilitation Project due to several reasons. When compared to satellite data, ground surveys and aerial photographs could be used to gather spatial information with a degree of accuracy. These traditional methods are costly, laborious and can not be used for investigation of unpredicted past event as the data collection has to be pre-planned. The coarse resolution of presently available satellite system can be offset with their capability of furnishing information of incidents that have been occurred in the past. Further, the synoptic view of the satellite data facilitates to observe an area as a whole giving the opportunity to multi disciplinary studies. The following were the main objectives of the remote sensing data analysis for the present project;

* Investigate the potentials of satellite data in volcanic damage assessment.
* Estimate the surface area of the pyroclastic and lahar flow after major eruption, and minor eruptions afterwards.
* Estimate the changes of pyroclastic and lahar flow with time.
* Investigate the changes in vegetation cover within the damaged areas, which will infer the surface condition of the area affected by the eruption.

Q.2 REMOTE SENSING SYSTEMS AND DATA MANIPULATION

2.1 SATELLITE SYSTEMS

Remote sensing is a process of obtaining information from a distance. These systems consist man made conventional cameras to high altitude satellite sensors. This section of the report enumerate the satellite remote sensing systems those could transmit information pertaining to earth, specially the state of the earth surface.

Present satellite systems that are mainly used in earth science are termed as passive systems except for radar satellite series that are grouped as active sensors. A passive sensor uses a energy source that is not originate from the satellite itself. In most of the cases sun serves as the energy source, and the reflected sun radiation from the earth surface is observed by satellite sensors and the observations are transmitted to receiving

station as the information of the corresponding place on the earth. The reflected energy from the earth surface is filtered at the sensor, and only the energy in pre-defined wavelengths are observed. Wavelength ranges have been established to suit for the scope of the satellite; land observation, weather, fisheries etc. Wavelength ranges are termed as *bands*, and they differ in number and wavelengths. The present satellite systems mostly use in the land based mapping are Landsat Thematic Mapper (TM), Landsat Multispectral Scanner (MSS), SPOT, Marine Observation Satellite (MOS), National Oceanic and Atmospheric Administration (NOAA) system, and recently launched radar systems, European Earth Remote Sensing system (ERS) and Japanese Earth Resources Satellite (JERS) series. The main characteristics of these satellites and their sensors are listed in Table 1.

NOAA gives the best repetition for monitoring with very coarse ground resolution for regional or country level information management. Landsat TM data gives the largest synoptic view with a single data set and it contains number of spectral bands suitable for multi-disciplinary applications. The MOSS data is similar to Landsat MSS in number of bands and the band wavelength, but has the poorest quantization level. Different sensors have their own merits and demerits. SPOT panchromatic (P) mode has the best surface resolution but information contained only in a single band.

Figure 1 shows the spectral response patterns of typical land cover classes and the average spectral radiance observed by some of the sensor spectral bands. Vegetation reflectance shows high variability. Low reflectance in the visible region of the spectrum accounts for the pigments in plant leaves. If a plant is subjective to some form of stress or damage that interrupts the growth decreasing the chlorophyll production, the spectral reflectance in the red band may increase. In the near-infrared of the spectrum the reflectance of vegetation increases dramatically, primarily due to internal structure of plants. Further, moving into higher wavelengths the reflectance decreases, and two dips in reflectance occur in the highly water absorption regions of the spectrum. The soil curve shows less variation in reflectance, hence less specific over spectral bands. Soil spectral response could change with the moisture content, texture, surface roughness, etc. and these will act on specific spectral region, such as moisture absorbed region.

It is important to note that a satellite data obtained for a particular area would give the status of the surface cover at the time of the observation. These observation may or may not give the current sate of the land use of the area.

2.2 *SATELLITE DATA*

Satellite data are distributed by mother agencies of respective systems and the authorized dealers distributed around the world. Receiving stations are located so that to assure the global coverage and to reduce the data storage capacity of satellite systems. Location of the receiving station for Landsat, MOSS, SPOT, and the contact information can be obtained from the respective authorized dealers.

The main draw back of the optical sensors those use reflected energy of earth surface is the presence of cloud cover. This is specially encountered in selecting data for countries in the tropical region. Therefore it is required to collect information of available data and the state of cloud cover for the required period before placing an order for satellite data.

The products available varies in data form and processing levels. Data can be purchased as photographic products for visual interpretation or digital products for digital and visual analysis. Either of these products can be ordered in Raw, System Corrected, or as Precise Geocoded products. Raw data needs corrections for variations in the satellite parameters, terrain, sun position etc. Corrected for satellite perturbations and mathematically transformed onto a geographical coordinate system are performed on system corrected data products. Precise correction involves system correction and

transformation into a given geographic coordinate system using map based ground control points. Cost of the products are varying with the required corrections.

Most of the digital data are sold in Computer Compatible Tapes (CCT). Spot data is available in CD-ROM, if requested. It is important to note that the CCT data format are depend on the mother agency and some cases differences can be found with receiving stations, even for same satellite system. Also, a request for a digital data set may take about two to three months and for a photographic product it may be little longer than that.

2.3 CONVENTIONAL DATA CLASSIFICATION METHODS

The digital satellite data classification can be addressed in two themes; visual interpretation and digital classification. As with photographic products digital data cane be printed in hard copy with image enhancement techniques to improve the quality and requirements of the work. This will give the layman to visually identify features by investigating color, texture and homogeneity. In contrast to visual interpretation, satellite data can be classified using digital classification methods resulting thematic maps. This procedure involves specialized hands and high computer processing time, but process data can be treated easily for map generation in different scales and integration with other digital products for multi-disciplinary studies.

If not transformed the digital values of satellite observation for respective ground irradiance with rigorous computations they can not be taken as absolute reflectance of a for particular surface cover. The computations for this conversion involves supplementary data pertaining to atmosphere, sun position and satellite position at the time of the observation.

The complex mathematical computation could be avoided in classification digital remote sensing data if a relationship could be established between the ground features and the corresponding digital data. This is the most popular technique used in digital data classification. The general statistical classification techniques are summarized and shown in Figure Q.2.

The process can be break into two major parts; Supervised Classification and Unsupervised Classification. The unsupervised classification is a result of grouping satellite data itself for the natural groups within the observation, mathematically. This may or may not correspond to interested land cover classes. In supervised classification reference information for interested land cover classes are collected at the time of the satellite pass. These information are compared with corresponding satellite observations in establishing mathematical or statistical relationships. Consequently, these relationships are used to classify the whole data set to the pre-selected land cover classes. The reliability of the final thematic maps are largely depend on the accuracy and the reliability of the reference information.

A combination of these two, referred to as Hybrid method in some literature is becoming popular as it consider the possible groups within a satellite data set before correlating with reference information. Ignoring the natural grouping within a satellite dataset in the process of surface reference information collection, classification could result unwarranted and unpredictable results.

2.4 HARDWARE AND SOFTWARE

It is clear that digital data have to be handled through computers as the satellite data are distributed in digital format recorded in CCT. Therefore a computer compatible tape reader is a must for any remote sensing analysis system. Consequently, the enormous data necessitate a large amount of computer disk space, for example a full scene of Landsat TM data that covers 180km x 180km occupies about 360MB of disk space. With these figures it is questionable to carry out analysis on a desktop computer as it may take

quite a long time to complete a job. The configuration of the software and hardware system used for the present work is shown in Figure Q.3. The shown configuration was selected to facilitate the integration of different types of data sources.

Q.3 STUDY AREA AND METHODOLOGY

3.1 OUTLINE OF THE STUDY AREA

The study area selected for the analysis is shown in Figure Q.4. This area covers the whole region that was damaged due to the eruption of Mt. Pinatubo except for small part in the South and West. Before the eruption the highest of the mountain was 1,745 m. above sea level. Eight river systems originate from Mt. Pinatubo. O'Donnell, Sacobia-Bamban, Abacan, Pasig and Gumain lies in the east of the volcano, and Tomas, Maloma, Marella and Maraunot-Balin drains to the west of Mt. Pinatubo. Some of these river network have been changed in the direction of flow, and some have divided forming new tributaries due to eruption.

3.2 DATA ACQUISITION

Comparing the ground resolution, quantization level and the multispectral characteristic of different satellite systems, and the requirements of the project, it was decided to carry out the work using Landsat TM data. The main characteristics and the fields of application of each TM spectral band is summarized and shown in Table Q.2. Landsat TM data are sold in pre-defined frames covering 180 sq. km. per dataset. These frames are identified as World Reference Coordinates. Special products covering 100 sq. km termed as Quarter Products are available from some of the selling agencies.

West Luzon, where the Mt. Pinatubo is located covers by two Landsat data frames having WRS numbers 116-049 and 116-050. Scene information obtained from EOSAT, Remote Sensing Technology Center of Japan (RESTEC) and the Thailand Remote Sensing Center (TRSC) pertaining to the TM data sets covering study area is shown in Table Q.3. Purchase of data was considered to cover the area of the Mt. Pinatubo Rehabilitation Project, and quarter products were ordered to reduce the cost. Cloud information are given for four quadrant of a frame, and the four columns in the tables represent the percentage of cloud cover for each of these quadrants. The quadrants that cover the study area are highlighted in the table. Landsat satellite system covers an area on the ground in every sixteen days permitting continuous observation. Theoretically, orbital characteristics of Landsat sensor assures two observations for a month of a given place. The tables shows that the presence of cloud cover in the area is considerable high throughout the year leaving only thirteen data sets are usable for the study for the period 1991 January to 1994 October. Among these data sets there was only two were with zero cloud cover. Comparing the availability of data with major volcanic activities in the area, datasets shown in Table 6 were acquired for the study.

Acquired satellite data and date of major volcanic activities

Year	Landsat TM data	Major Eruptions
1990	1990.01.20	
	1990.07.15	
1991		June 12 - 17
1992	1992.02.11	
		Apr. 4
	1992.06.18	
		July 13
	1992.10.08	Sep. 20-21
	1992.11.25	Nov. 20-24
1993	1993.02.13	
	1993.04.02	
	1993.07.07	
		Oct. 5-6
	1993.12.30	
1994	No data	

There are some datasets that could not use to cover the whole study area due to presence of cloud cover. Some of the datasets in the table were selected after consultation with the experts in the handling agency, and comparing cloud cover present in the area of interest.

3.3 PROCEDURE OF ANALYSIS

The area of the analysis was selected referring to the pyroclastic and lahar damaged area published by the Department of Public Works and Highway (DPWH), and shown in Figure Q.5. Pyroclastic deposit after eruption, lahar flow at the end of 1991 and in the following years are shown separately. The criteria of the analysis is shown in Figure Q.6. The analysis could be discussed in three major steps; Pre-processing, qualitative analysis and quantitative analysis.

The pre-processing is performed to rectify the satellite data orientation into a common map projection for easy comparison and to maintain compatibility with other data pertaining to the study. The process is referred to as georeferencing. In qualitative analysis, the best suitable spectral bands were selected for enhancement of the damaged areas due to pyroclastic and lahar flow. Enhanced images were produced and the visual interpretation was carried out. In visual interpretation DPWH estimation was used as interpretation key and the area of pyroclastic and lahar deposit and changes were compared with respect to DPWH survey report.

In quantitative analysis, attempt was made to estimate the damaged area due to eruption using digital techniques. Pyroclastic and lahar flow deposited areas were digitally identified, delineated and compared with the DPWH estimations. The damage extent was estimated and compared with DPWH prediction for accuracy estimation. Further, the changes in these areas were observed using vegetation index to quantify possible changes in the process of recovery.

3.4 PRE-PROCESSING OF SATELLITE DATA

In pre-processing, all the satellite datasets were georeferenced using maps in 1:50,000 published by National Mapping and Resource Information Authority. Universal Macerator Coordinate system was used in the process to maintain data compatibility with other digitized information of the project. First order coordinate transformation for georeferencing, and Nearest Neighbor method for re-sampling was used in the rectification process. Highly distributed ground control points were selected in order to

reduce the error in spatial matching, and the average root mean square error was less than one pixel unit in TM data.

Q.4 QUALITATIVE ANALYSIS OF VOLCANIC DAMAGE

Data sets were not available for the year 1991 and the number of usable acquisition for the present work was relatively few in number. Among the datasets acquired for the analysis, two sets were not suitable for quantitative analysis due to amount of cloud cover, and the remaining six data sets were used in quantitative and qualitative analysis. Partial cloud cover was present in four data sets used for the analysis. The purchased datasets supposed to be the best for the area acquired by the TM sensor for the last few years.

Image processing was carried out using the georeferenced datasets to produce best possible enhancement for visual interpretation of the TM data. Depending on the extent of pyroclastic flow and the cloud cover, the visual contrast of the images were highly varying as the reflected energy levels were different. Linear stretch and histogram equalization was used as enhancement techniques in the image processing. It was observed that TM band 1, 2 and 3 could permit relatively better enhanced images for qualitative analysis as this combination is more realistic to human eye. Color composites of the enhanced images were produced for each date assigning band 1, band 2 and band 3 to blue, green and red color components, respectively. Images were produced for the whole area, and enlargements for some selected areas. Interpretation was carried out on these images, and the discussion follows is cross referenced with the river network of the area, figure Q.4.

Figure Q.7 to Q.12 shows the whole study area before and after eruption. Also, these six images can be further grouped into two seasons; wet and dry. Cloud cover present in satellite data is highlighted in yellow. Figure Q.8, Q.10 and Q.12 belongs to the wet season and the remaining three to the dry season. The seasonal differences in the area are clearly visible in the pre-eruption images shown in Figure Q.7 and Q.8 for 1990 January and 1990 July, respectively. High seasonal changes is observed in the western part of Mt. Pinatubo, where the land cover is either grass or scrub. Further, diminished green cover in the 1990 January image is visible in the entire area showing seasonal changes in grass lands, forest cover and cultivation pattern in the area. Light blue tone represents developed areas, and can easily be compared with the location of Angeles City. Relatively high reflectance can be observed in the vicinity of Clark Air Base in both pre-eruption images, and this brightness is similar to bare lands and river wash areas in the study area. The bright colors in the low land area bordering Angeles City of January 1990 image could be interpreted as agricultural areas as these areas in the wet season image indicates high amount of green color. Also, considering the texture and pattern in these areas with their spatial location, these areas can estimated as agricultural lands. In the dry season these areas show similar spectral pattern of river wash and other bare lands. These two pre-eruption images represent the status of area before the eruption with seasonal characteristics.

Figure Q.9 shows the devastation due to the volcanic eruption. Though this has been acquired on 1992 February 11th, the damage due to eruption is quite visible, even after considerable time. Bright white color represents pyroclastic and lahar deposits. The extent of the lahar deposit in Santo Tomas, Balin-Baquero, Sacobia, Bamban, Pasig and Gumain rivers is clearly visible. The destruction due to ash fall is observable and this could have damaged most of the vegetation in the vicinity of Mt. Pinatubo. The damage due to ash fall is severe in the western part than the damage to east of the mountain. Also, the northern part of the mountain is not affected by the ash fall. The bright white color in the south of Clark Air Base could be the abandoned or un-cultivated agricultural lands, and the discrimination of them from ash fall areas was quite complicated.

When compared with Figure Q.10, which has been acquired on November same year it is clearly visible that some of the ash deposits near the peak has been washed out. An increase or a deviation of lahar flow is visible at the upper stream of Bamban River. This could have happened due to secondary explosions that might have triggered during the rainy season, or lahar and mudflow due to considerable precipitation experienced during the July and August 1992, Table Q.5. The ash deposits in the western mountain ranges does not show much change.

Figure Q.11 shows the status of 1993 April but does not account for appreciable changes. During November 1992 to April 1993 neither major volcanic activity nor heavy rainfall has been occurred in the area.

1993 December image shows evidence of changes in the vegetation close to the crater of Mt. Pinatubo. The ash deposit in the vicinity of the peak has been cleared and the lahar flow is concentrated in the streams. Diminishing white color in the peak of the mountain could be due to the decrease of the pyroclastic deposit. This decrease is only visible near the crater of the volcano. The deposit in the mountain slopes do not show any changes as with the deposits in the top. The red-brown color of the mountains to west of volcano indicates the recovery of them from the initial ash deposit. Visual observation shows the lahar deposit has been increased near the city of Bamban, but certain decrease of the spread in the downstream of the Bamban River.

Further, the visual interpretation was carried out using enlarge prints of selected areas. Three areas were selected for detail observation and the enhanced images are shown in Figure Q.13 to Q.15, representing north-west, north-east and south-east of the Mt. Pinatubo peak. Figure Q.13 shows part of Balin-Baquero river. The pre-eruption images show the land cover of the area and their seasonal changes. The 1992 February image account for the damage due to eruption and most of the vegetation up to Balin-Baquero river. Mountains in the upper left of the figure was not affected indicating the ash flow was not directed northward. Recovery of the area with time is depicted in the remaining images. Images acquired in different seasons could not be easily comparable, but having the knowledge of the land cover presence in the area reasonable judgment of the changes could be made. As indicated earlier, the depth of the pyroclastic deposit might have decreased in the peak but remains in the slopes. The increase of vegetation in 1993 December image indicates the westward mountain slopes could stand for possible soil erosion.

The observation of the north-east image shown in Figure Q.14 is similar to that of Figure Q.13. Decrease of ash deposits and possibly the depth of pyroclastic deposit is visible. The extent of the pyroclastic deposit remains same.

Figure Q.15 shows the devastating impact of ash fall in the eastern slope of Mt. Pinatubo and the recovery. Though the cloud cover in the 1993 December image obscure the interpretation, remarkable recovery could be observed in the vegetation in the mountain slope.

Qualitative analysis of the images produced by image enhancement techniques clearly shows the recovery of vegetation in the mountain slopes. Further, the diminishing bright white color in the peak could interpret for decrease of the pyroclastic flow in the close vicinity of the summit. Also, the lahar flow is concentrated in the river net work needing further counter measures against flood and lahar flow. The mountain slope could be considered as stable, specially the west to Mt. Pinatubo, and may not very much vulnerable for erosion as a certain degree of vegetation recovery can be seen.

Q.5 QUANTITATIVE ANALYSIS OF DAMAGE AND CHANGES

The source of satellite data is described in previous section, and it is clear that the energy receives at a sensor depends on the amount that is reflected from ground surfaces.

Further, the reflected energy is a function of the irradiance and the reflectivity, where the irradiance depends on the position of the sun and the climatic conditions. Seasonal variation of the sun position could influence the irradiance at the ground and it is difficult to compare data observed in different seasons unless establishing the amount of radiation at the time of the observation. Transformation of satellite observed radiance into corresponding amount of reflected energy, specifically sensor digital counts into reflected energy can be carried out using sensor calibration equations and atmospheric models. Sensor calibration reports and calibration coefficients can easily be acquired, but the atmospheric parameters that necessary in an atmospheric model are rarely visible. In the present work these data were not obtainable as reliable observation of visibility, temperature, moisture content etc. are not available for the area of the coverage. further, the atmospheric scattering in this area could relatively higher after eruption due to excessive discharge during the eruption. Also, the background reflectance could have contributed higher than in a common datasets due to the large extent of bright lahar and pyroclastic deposit present in the area.

5.1 DAMAGE ASSESSMENT DUE TO MT. PINATUBO ERUPTION

1992 February data set was used for digitally estimate the devastation of the eruption and the disturbance that have been occurred in the area. Initially, the TM bands digital counts for lahar and pyroclastic deposited areas and the rest were extracted for estimation of spectral discrimination. Figure Q.16 shows the average spectral response patterns of Landsat TM bands of pre-defined areas on the image. Selected cover classes for investigation of spectral discrimination were; pyroclastic in the vicinity of summit (pyro-summit), pyroclastic and lahar deposit in mountain slopes (pyro-slope), lahar deposits in river beds (lahar-wet), ash fall deposited areas (ash), partial damaged vegetation (vege-damage), agricultural lands (agri), and developed lands. Highest spectral discrimination of these classes was observed in TM band 1 to band 5. Thematic Mapper Band 6 response range was very narrow and the spectral discrimination using thermal emission was not considered. The mean digital counts for pyroclastic deposit on the summit and on the slopes were quite dissimilar, but discrimination was hindered due to high variation in digital counts. There was no spectral difference in lahar and ash fall to facilitate digital discrimination of these two. Observing the patterns and the possible discrimination potential of surface classes it was decided to continue the classification using digital counts of first four TM bands. As with the normal soil curve discussed in the previous section the lahar, pyroclastic and ash deposits do not differ in their spectral responses as far as the surface materials remain the same.

Visually observing the color composite, samples regions were extracted for classification. Number of regions were selected for cover classes that showed higher spectral dissimilarities to prevent spectral variation within the region. Lahar in dry and wet areas, pyroclastic in summit, east slope, west slope, ash fall deposit, vegetation damaged are some of the regions established for evaluate the volcanic damage.

Digital counts of Landsat TM bands were extracted for the regions established above, required statistical parameters were calculated, and classification was carried out using Maximum Likelihood algorithm. The resulted image was observed for discrimination of defined categories, and it was found that the region separation was poor in most of the ash fall areas, lahar in dry areas an d pyroclastic flow in mountain slopes. Further, the discrimination of bare lands and the damage vegetation was poor. As the spectral similarities are inherent properties of these classes the results may not be improved even with different statistical classification approaches. To over come this situation it was decided to use digitized river network of the area to discriminate the inter-class overlap and extract the pyroclastic and lahar deposited extents.

The rivers that are originated from Mt. Pinatubo and their tributaries were identified visually. Buffer zones were created for these rivers that could fill during the lahar flow. Major rivers were assign 1500 meter buffer zone and minors were given 150 meters. The

buffer sizes were decided on investigating the topographical maps of the area, and visual investigation of TM images.

Integrating this geographical information with the classified satellite data the pyroclastic and lahar deposit as at February 1992 was delineated, Figure Q.17. The DPWH estimates shown in Figure Q.5 were digitized and incorporated in the GIS database for comparison of satellite data classification. The total damage area estimates according to DPWH surveys is shown below;

DPWH estimates of pyroclastic and lahar deposit

91 Pyroclastic	91 Lahar	92 Lahar	93 Lahar
163.9 sq. km	313.9 sq. km	42.42 sq. km	12.9 sq. km

Satellite data estimated lahar and pyroclastic deposit extents were compared with the DPWH extents, and summarized as shown below. It was not possible to separate pyroclastic and lahar flow from satellite data, and they were shown as one group in satellite data analysis.

Comparison summary of DPWH and TM estimation for 1991 damage

TM Estimate	DPWH Estimate		
	Pyroclastic	Lahar	Non Damaged
Pyro & Lahar	133.5 sq. km	139.2 sq. km	168.5 sq. km
Non Damaged	30.9 sq. km	105.7 sq. km	

Considerably high discrepancy is observed between DPWH and Landsat data estimations. In TM data classification an area of 169 sq. km has been added to the total damaged area that was not identifies by DPWH investigators. Also, 106 sq. km identified as lahar deposited areas by DPWH surveys was not classified as damaged areas by satellite data analysis.

Graphical representation of the DPWH and TM classification is shown in Figure Q.18. This figure reveals the accuracy, agreement and dissimilarities of interpretation of both of the sources. Higher extent of pyroclastic deposits have been classified by remote sensing data in the vicinity of the crater. Further, scattered distribution of damaged areas are found along narrow streams around Mt. Pinatubo. In remote sensing data estimation, the crater has been classified as pyroclastic deposit as the spectral reflectance of crater that is covered with ash could have been similar to that of pyroclastic deposits. The higher damage estimation of DPWH is found in the vicinity of down stream of Abacan River, Bamban River, Gumain River, Pasig River. Attempt was made to investigate the discrepancy by comparing the two estimations in the areas where higher degree of dissimilarity is observed.

Areal differences of the locations that showed high discrepancy were evaluated for investigate the reasons for differences. Extents were estimated for both of the sources for areas depicted by squares in the Figure Q.18 and shown below;

Areal differences between TM and DPWH estimation for defined locations
(area represents in sq. km)

	crater	Bamban	Abacan	Pasig	Gumain
DPWH	43.7	48.2	19.3	34.0	10.9
TM	88.9	3.8	0.3	6.6	1.3
Difference	-45.2	44.4	19.0	27.4	9.6

Along the down streams of the rivers discussed above, the DPWH estimations are higher than TM, totaling a difference of 100 sq.km. This could account for the discrepancy of

satellite data classification of the DPWH estimated damaged areas as non-damaged. In the vicinity of the crater in the survey of the later. This could explain for a part of the higher estimation of damaged area by TM data.

The un-explained differences of the two sources could be due to number of factors, some of which are inherent properties of data sources and others could be natural phenomenon occurred between the time span of the source data. The extent comparison was carried out digitally using the digitized process due to sensitivity of the digitizer as most of the features were linear. Unlike TM data, which have same spatial accuracy and resolution for the whole area, the DPWH data might have acquired from various sources that could have different degree of accuracy and reliability. Further, the time difference of data sources might have induced the discrepancy in the comparison.

5.2 CHANGE ANALYSIS BY MULTI-TEMPORAL SATELLITE DATA

Attempt was made to estimate the temporal changes of pyroclastic and lahar flowing using Landsat TM data for the period of February 1992 to December 1993. Time series analysis was carried out using five datasets acquired in November 1992, February 1993, April 1993 and December 1993. The analysis was carried out to estimate the reliability of pyroclastic area estimation by Landsat TM datasets, and to detect the areal changes of pyroclastic and lahar deposit during the period of the available satellite data.

Figure Q.19 and Q.20 shows he spectral response patterns for pyroclastic and lahar flow deposited in various spatial locations. It is quite visible that there is a spectral similarity between different surface features, and spectral dissimilarities for same feature of land cover with the change of spatial locations. Also, comparison of these figures shows that there is a spectral variation in the two dates data sets. This dissimilarity in the digital count hinder establishing global statistical formula for discriminating lahar and pyroclastic flow for data acquired in different time of the year. Due to this reason, data classification was carried out by the method described in the previous section by independently classifying Landsat datasets. Reference regions were selected for pyroclastic, lahar and other categories on each Landsat data set by visual observation of color composites. Each dataset was treated with Maximum likelihood classification method in the process of classification. Un-affected areas were not considered in the classification, and these areas were grouped into a single class during the process. As with the February 1992 dataset the class mixture was observed. The river network information was incorporated as described earlier in estimating pyroclastic and lahar deposit of each classified Landsat dataset. The results of the temporal analysis are shown in Figure Q.21, and the areal extents are shown below;

Estimation of pyroclastic and lahar deposited areas by Landsat TM data
(figures represent areas in sq. km.)

Date	1992 February	1992 November	1993 February	1993 April	1993 December
Extent	441.8	448.8	373.1	362.3	406.1

Pyroclastic and lahar deposits in February 1992 and November 1992 are almost similar. Consecutive decrease is observed in the time between November 1992 to February 1993 and February 1993 to April 1993. The later decrease, which is comparatively low has been occurred during the dry season. This could be considered as erroneous estimate due to ground resolution of TM sensor. If the reflectance of a certain material shows considerable contrast to the surrounding, possibility exits to extract the surface information of the bright features even its areal extent is smaller fraction of the TM ground resolution. Change of deposit between November 1992 and February 1993 is appreciable and could be due to washed out of pyroclastic deposits. Also, the decrease can be account for the vegetation that have recovered after the eruption, specially in mountain slopes. The increase of deposit at the end December 1993 could be due to

excessive rainfall experienced during the rainy period of the same year, Table 4, 5 and 6. This comparison shows the state of the within two dates, but does not reveal the spatial location of the changes. Therefore, attempt was made to identify the changes of damaged area between each set of Landsat data. The changes estimated area graphically shown in Figure Q.22.1 and Q.22.2 and summarized below;

Changes of pyroclastic and lahar deposited area estimated by TM data
(area represents in sq. km.)

Time span	no change	increase	decrease
92-February to 93-February	304.6	66.8	134.4
92-November to 93-December	328.3	74.2	92.1
92-February to 93-December	294.2	107.5	144.8
93-April to 93-December	305.4	93.8	52.4

The interpretation of the above observation is quite intricate as decreases as well as increases in the extent of pyroclastic deposit has been undergone in the same time. The total unchanged area remained almost same, and this area may represents the thick pyroclastic and lahar deposited areas in the mountain slopes and river beds. Changes in these areas may not occur within a short time span as considered in this analysis. Figure Q.22.1 and Q.22.2 shows that the changes are mainly occurred in down streams and narrow tributaries where the changes are mainly due to the excessive rainfall. The climatic condition of this area may contribute for the changes in the deposited extents and may be required to further investigate the area in watershed basis.

The Landsat TM data estimates were compared with the DPWH estimates for lahar deposits of 1992 and 1993. DPWH estimate of 92 lahar was compared with 1993 February TM classification, and 93 lahar area was compared with the December TM dataset of the same year. The results are graphically shown in Figure Q.23.

5.3 CHANGE ASSESSMENT IN WATERSHED BASIS

Volcanic damage in the area as a whole and the changes of the pyroclastic and lahar deposited extent in the affected areas was discussed in the previous section. The changes of pyroclastic and lahar deposit could be due to secondary explosions or as result of heavy rains. These phenomenon and climatic factors could be spatial dependent, and investigation of damage extent and changes in area basis could reveal locational characteristics of extent of deposit and the changes.

The study area was subdivided into four zones considering the distribution of river network and the extent of lahar and pyroclastic deposit. The subdivided sections are named as North Zone, East Zone, South-West Zone and South Zone as shown in Figure Q.24. Further, the destruction and the change was investigated in the slopes of Mt. Pinatubo depicted by broken lines in the figure. Also, zone investigation was carried out for changes of pyroclastic and lahar deposit in the mountain slopes depicted in the figure. Summary of the observations or the whole study area in zone basis is shown below;

Distribution of satellite data estimated damage extents in defined zones
(figures represent extents in sq. km)

	1992 February	1992 November	1993 February	1993 April	1993 December
North Zone	50.9	54.9	48.1	46.5	44.7
		(-8%)	(5%)	(8%)	(12%)
East Zone	157.7	166.6	122.4	118.5	149.5
		(-5%)	(22%)	(25%)	(5%)
South-West Zone	94.6	86.6	74.9	72.1	82.8
		(8%)	(21%)	(24%)	(12%)
West Zone	138.6	140.7	127.6	125.2	129.1
		(-2%)	(8%)	(10%)	(7%)

Figures under each date represents the deposit area and the figures within brackets show percentage of the change with respect to the extent of February 1992. November 1992 extents are higher than February extents of the same year except for South-West zone. This shows that the 1991 rainy season has affected the pyroclastic deposit in the whole area increasing the areal coverage except for south-west. Continuous decrease is found in the North zone afterwards with a constant percent of decrease in each year. There is only a single major river is located in this zone hence, the change of lahar due to rainfall could have been minimum in this areas. The South-West zone showed the highest recovery up to April 1993, but the rainy season followed would have re-captured the recovered area. In general, the extents of the lahar deposit is decreasing, but have to be carefully observed during rainy season.

Similarly, the changes of the lahar and pyroclastic deposits in the mountain slopes were observed and summary is shown below;

Distribution of satellite data estimated damage extents in defined zones
(figures represent extents in sq. km)

	1992 February	1992 November	1993 February	1993 April	1993 December
North Zone	31.1	25.1	21.7	21.7	21.6
		(24%)	(32%)	(32%)	(13%)
East Zone	46.9	42.3	34.1	34.9	32.7
		(2%)	(2%)	(25%)	(30%)
South-West Zone	48.4	43.4	38.0	36.9	30.9
		(10%)	(21%)	(24%)	(36%)
West Zone	126.4	127.0	114.5	112.7	109.7
		(0%)	(9%)	(11%)	(13%)

General trend of the change is similar to the whole study area, but the percent of change is quite higher in mountain slopes. Except for the West zone, other zones have showed about 30% decrease in deposited area. Also, the figures indicate that the change is diminishing with time as the remaining voluminous deposits in river beds may not show change within a short time span. Considerable decrease in early stage could be due to the washed out of lahar in mountain slopes. Further, the changes in the mountain slopes do not show any increase, hence, the increase of deposits in the study area may have taken place in the down stream.

Q.6 ASSESSMENT OF VEGETATION RECOVERY

In pyroclastic and lahar deposit change assessment it was observed that extents of some damaged areas were decreasing, specially in mountain slopes. This decrease could a sign of the stability of pyroclastic and lahar deposits, and more un-stable deposits may have washed out. The stable deposit areas may be concentrated in the river beds, and the other slopes that were disturbed by the eruption may have recovered their past state. Attempt

was made to investigate for any sign of re-growth in the vegetation cover in areas where the decrease of pyroclastic and lahar deposits was taken place.

Normalized Difference Vegetation Index (NDVI), generally known as NDVI was used as interpretation key, which is one of the most popular index in the vegetation type mapping, vegetation stress evaluation, vegetation and non-vegetation mapping, etc. Also, this is used to investigate vegetation in large areas as it localizes the differences due to view angles, terrain and atmospheric condition at the time of the satellite pass. The commonly use mathematical formula for NDVI is;

$$NDVI = \frac{\text{Near Infrered - Visible}}{\text{Near Infrered + Visible}}$$

for TM sensor;

$$NDVI = \frac{\text{TM band 4 - TM band 3}}{\text{TM band 4 + TM band 3}}$$

Clouds, water have higher reflectance in the visible region than the infrared region resulting negative NDVI values. Vegetation reflectance in the near infrared region is higher than visible region accounting for positive higher values of NDVI for vegetation. Densely vegetation will have the highest NDVI. Soil, and bare lands reflectance in these two bands are similar, hence the NDVI values would be near zero.

To avoid the effect of seasonal changes in the TM digital counts the NDVI interpretation was carried out with datasets acquired during the same season of the year. Comparison was done for the time interval of November 1992 to December 1993 and February 1992 to February 1993. Pyroclastic and lahar deposited areas of February 1992 was extracted, and the NDVI values of February 1993 was investigated to identify the areas for increase in vegetation cover during the time span of the two datasets. Similarly, November 1992 data was compared with December 1993 to identify the areas of vegetation recovery.

The following NDVI values were established after extracting sample data from undamaged areas of the TM data sets. The cover classes established for NDVI representation are bare lands, grass lands, forest low-density and forest high-density. The NDVI ranges observed for these classes can be listed as follows:

Distribution of NDVI values for identified land cover classes

Bare lands	Grass lands	Forest low-density	Forest high-density
NDVI < 0.2	0.2 < NDVI < 0.4	0.4 < NDVI < 0.6	NDVI < 0.6

In reality the NDVI values are changing with the density of canopy cover making it difficult to establish ranges for various land cover classes. The NDVI values are related to the density of the canopy, chlorophyll concentration, and not with the land cover classes. But, the characteristic nature of the growth and the structure of the canopy could make the use of NDVI for differentiate vegetation classes. Given this explanation, the cover classes above are most suitable for the defined NDVI ranges for the study area.

These ranges were established after extracting sample defined on each datasets. Extracted samples were statistically analyzed for establishing ranges using mean values and standard deviations. NDVI ranges were applied and the regeneration of vegetation cover within the pyroclastic damaged areas were investigated for the datasets described above. Graphical representation of the result is shown in Figure Q.25. The increase in the amount of NDVI is represented by the typical land cover classes in the study area as explained above. Frequency distribution of satellite observed data points for the four zones defined in the previous section is shown in Figure Q.26 and Q.27 for the changes

observed for February 1992 to February 1993 and November 1992 to December 1993 datasets.

Increase of vegetation cover for grass and low density forest estimated by NDVI for the period February 1992 to February 1993 (figures are given in hectares)

	North	East	South-West	West
Grass	280	267	187	352
	(9%)	(5.7%)	(3.8%)	(2.8%)
Forest low-density	38	98	16	3
Forest high-density	0	0	0	0

Increase of vegetation cover for grass and low density forest estimated by NDVI for the period November 1992 to December 1993 (figures are given in hectares)

	North	East	South-West	West
Grass	229	237	201	537
	(9%)	(5.6%)	(5%)	(4%)
Forest low-density	33	50	37	42
Forest high-density	0	0	0	0

The figures are given in hectares for increase in vegetation for each land cover class. Further, the values in brackets represents the percentage recovered with respect to the damaged area in each zone. The comparison identifies the growth in green cover of the damaged area established on the old dataset for both of the comparison. The above result shows that the highest recovery is observed in the West zone for both comparison and least recovery in the south-west direction. In general terms, the percentage of recovery is higher in the eastern slope of the mountain than the western slope. In either case the recovery is in the very low vegetation range with NDVI range representing grass lands. Comparatively higher recovery in the low vegetation category is seen in the wet season, and this classification could be due to seasonal changes in the vegetation itself. Therefore, the changes in both of the dates could be considered as very similar, and as a whole the percentage that has recovered is not very significant. The sign of re-growth in the vegetation is shown indicating stability of mountain slopes are increasing.

Q.7 COMMENTS AND RECOMMENDATIONS

7.1 ACCURACY OF CLASSIFIED REMOTE SENSING DATA

Discussion of accuracy is a relative process based on a given true information. In the present analysis the remote sensing investigation was compared with surveys carried out by aerial photograph interpretation and field visits. There is basic difference in these two type of analysis. The DPWH interpretation, which was considered as the true information is highly subjective, and the state of the interpretation could change with the interpreter. In contrast, the remote sensing classification is an objective process, and the results may not be differ with the analyst. Therefore, the comparison of these two different source of information may be carried out subjectively, rather than comparing areal extents to establish the suitability of remote sensing data.

The resolution of remote sensing data could yield unwarranted results due to class mixture within a given pixel. Also, highly reflective feature within a pixel could hinder the information of the surrounding even the particular feature represents smaller areal extent. This phenomena might have caused some undamaged areas to be mapped as damaged areas in the present study. Generally, suitability of remotely sensed data for present kind of surveys is highly recommendable, and the future high resolution sensor may provide much more detailed explanation for similar works.

7.2 RECOMMENDATION FOR FUTURE WORKS

It is observed that remote sensing data can satisfactorily be used in pyroclastic and lahar damaged assessment. Also, potential of satellite data in time series analysis is un-matched with any other land information system available at present. Changes are observed in the study area in the recovery of vegetation, and continuous observation in this aspect would lead better planning of infrastructure for mitigation of future mud and lahar flow. State of watersheds in the region could serve as an index for the rehabilitation of the area in a global context, and remote sensing data can contribute to monitor the changes timely and economically.

TABLES

Table Q.1 Characteristics of commonly used satellites and their sensors

	Landsat	MOSS	SPOT	SPOT	NOAA
Sensor	TM	MESSR	HRV-XS	HRV-P	VAHRR
Spectral Bands	7	4	3	1	3
Orbit Type	Sun Syn.	Sun Syn.	Sun Syn.	Sun Syn.	Sun Syn.
Inclination	98.25	99	98.70	98.70	98.80
Nominal Altitude	705km	909km	832km	832km	854km
Swath Width	185km	100km	60km	60km	3000km
Recurrent Period	16 days	17 days	3-4 days	3-4 days	every day
Ground Resolution	30m	50m	20m	10m	1.1km
Quantization Level	8 bit	6 bit	8 bit	8 bit	10 bit

Table Q.2 Major fields of application of the Landsat TM spectral bands

Band	Wavelength	Nominal Spectral Location	Principal Application
1	0.45 - 0.52	Blue	Coastal water mapping Soil vegetation discrimination
2	0.52 -0.60	Green	Vegetation discrimination Vigor assessment
3	0.63 - 0.69	Red	Plant species discrimination Plant vigor assessment
4	0.76 - 0.90	Near-Infrared	Biomass assessment Moisture estimation
5	1.55 - 1.75	Mid-Infrared	Vegetation moisture Soil moisture
6	10.4 - 12.5	Thermal Infrared	Vegetation stress Soil moisture. Thermal mapping
7	2.08 - 2.35	Mid-Infrared	Mineral and rock type discrimination Vegetation moisture assessment

Table Q.3 Landsat Thematic Mapper Data Information

116-049				116-050				Date
3	8	0	5	1	9	1	8	17.01.89
8	8	7	6	5	8	4	8	02.02.89
1	4	1	3	1	4	1	7	18.02.89
9	9	9	9	9	9	7	6	06.03.89
9	9	9	9	9	9	8	9	22.03.89
9	9	9	9	3	4	1	6	07.04.89
8	8	5	5	3	4	2	5	23.04.89
7	6	6	5	5	7	3	7	09.05.89
6	9	8	7	7	7	1	7	25.05.89
8	7	7	6	8	6	8	8	10.06.89
5	6	8	5	8	5	2	7	26.05.89
4	7	0	3	4	7	4	4	01.11.89
5	9	0	3	0	6	2	6	17.11.89
1	3	0	3	0	3	0	2	03.12.89
9	9	9	9	9	9	8	8	19.12.89
5	7	1	3	1	8	2	9	04.01.90
5	8	0	7	1	7	2	7	20.01.90
2	6	0	2	1	5	0	5	05.02.90
0	4	0	7	0	7	1	6	21.02.90
7	9	9	9	9	9	9	9	09.03.90
2	2	0	4	2	4	1	6	25.03.90
0	2	1	5	4	9	1	9	10.04.90
5	8	3	9	3	8	1	6	12.05.90
9	9	9	0	9	8	8	7	28.05.90
8	8	7	7	8	7	5	6	13.06.90
9	9	9	9	9	9	9	9	29.06.90
0	3	1	5	0	6	3	2	15.07.90
9	9	9	8	9	9	7	7	18.07.91
9	9	9	8	7	6	1	5	03.08.91
9	5	9	8	9	9	9	9	19.08.91
9	9	9	9	9	9	9	9	04.09.91
9	6	9	9	9	9	9	9	20.09.91
7	6	7	3	5	5	7	6	06.10.91
7	9	9	9	9	9	9	9	22.10.91
5	9	8	9	9	9	7	9	07.11.91
5	9	6	9	7	8	5	7	23.11.91
9	9	0	5	0	3	1	1	26.01.92

Table Q.4 Daily Rainfall in Sacobia River Basin in 1991

Station: SACOBIA
Year: 1991
Agency PHIVOLCS

(Unit : mm)

	Jan	Feb	Mar	Apr	May	Jun	Jul	Aug	Sep	Oct	Nov	Dec
1									0	2	0	0
2									0	1	15	8
3									0	0	0	0
4									0	7	8	0
5									0	1	0	0
6									0	30	0	0
7									0	1	0	0
8									0	4	0	0
9									0	0	0	0
10									38	0	0	0
11								0	0	0	0	0
12								0	0	0	0	0
13								0	6	10	0	0
14								0	15	57	0	0
15								0	50	21	0	0
16								0	77	0	0	0
17								0	36	54	0	0
18								0	27	2	93	0
19								0	80	0	40	0
20								0	32	0	0	0
21								0	17	0	0	0
22								0	22	3	0	0
23								0	2	0	0	0
24								0	0	0	0	0
25								0	0	0	0	0
26								0	0	0	0	0
27								0	0	0	0	0
28								0	9	0	0	0
29								0	0	65	0	
30								0	21	4	0	
31								0		0		
Total				0	0	0	0	0	432	262	156	8
											Annual Total=	858
Daily Max	0	0	0	0	0	0	0	0	80	65	93	0
RainyDay				0	0	0	0	0	14	15	4	1

Table Q.5 Daily Rainfall in Sacobia River Basin in 1992

Station: SACOBIA
Year: 1992
(Unit : mm) Agency PHIVOLCS

	Jan	Feb	Mar	Apr	May	Jun	Jul	Aug	Sep	Oct	Nov	Dec
1					0	0	26	4	48	0	15	
2					0	0	2	0	42	0	1	
3					0	34	3	11	10	0	0	
4					0	12	0	30	0	0	0	
5					0	0	0	2	0	0	0	
6						0	0	26	0	0		
7						7	0	3	0	0		
8					0	0	0	1	0	0		
9					0	0	0	0	0	0		
10					41	0	0	18	0	0		
11					0	0	81	2	0	0		
12				54	0	0	3	0	0	0		
13				0	0	0	83	1	0	0		
14				7	0	0	2	11	0	0		
15				0	0	3	3	43	0	0		
16				11	0	0	10	26	0	10		
17				0	0	5	0	22	0	59		
18				0	0	0	26	53	0	1		
19				0	0	8	3	45	0	5		
20				0	38	5	37	65	0	10		
21				0	0	0	47	46	0	22		
22				0	11	0	1	4	0	0		
23				2	1	13	4	0	0	11		
24				0	0	2	2	18	0	0		
25				0	0	2	0	10	0	19		
26				0	0	16	12	13	0	57		
27				0	0	60	39	41	0	4		
28				0	0	22	34	157	0	0		
29				0	0	3	1	232	0	0		
30				0	0	3	37	59	0	0		
31					0		1	62		0		
Total				74	91	195	457	1005	100	198	16	
										Annual Total=		2136
Daily Max	0	0	0	54	41	60	83	232	48	59	15	
RainyDay				4	4	15	22	27	3	10	2	

Table Q.6 Daily Rainfall in Sacobia River Basin in 1993

Station: SACOBIA
Year: 1993
(Unit : mm) Agency PHIVOLCS

	Jan	Feb	Mar	Apr	May	Jun	Jul	Aug	Sep	Oct	Nov	Dec
1	0	0	0	0	0	0	0	0	1	2	16	0
2	0	0	0	0	0	0	105	0	6	36	132	10
3	0	0	0	0	0	0	0	0	19	3	1	2
4	0	0	0	0	0	0	0	62	29	30	0	0
5	0	0	0	0	0	30	2	3	45	370	0	0
6	0	0	0	0	0	0	1	1	0	33	0	2
7	0	0	0	20	0	0	0	34	35	50	0	3
8	0	0	0	34	0	3	0	3	27	0	0	0
9	0	0	0	0	0	20	5	1	4	14	0	0
10	0	0	0	0	0	0	1	14	0	0	0	0
11	0	0	0	0	41	0	0	0	0	0	0	0
12	0	0	0	0	0	0	0	34	0	0	0	0
13	0	0	0	0	0	0	0	51	0	0	0	0
14	0	0	0	0	0	0	0	4	0	21	0	0
15	0	0	0	7	0	43	39	1	0	34	0	0
16	0	0	0	0	0	37	10	2	0	2	15	10
17	0	0	0	11	0	0	0	28	0	0	0	1
18	0	0	0	0	0	0	0	1	0	0	0	0
19	0	0	0	0	0	0	16	306	0	4	0	
20	0	0	0	0	0	0	0	2	0	0	0	
21	0	0	0	0	0	0	7	4	43	0	0	
22	0	0	0	0	38	0	8	0	0	0	4	
23	0	0	0	0	11	0	0	0	0	0	0	
24	0	0	0	0	0	11	10	1	0	0	0	
25	0	0	0	2	1	0	7	0	0	0	0	
26	0	0	0	0	0	235	5	0	8	0	0	
27	0	0	0	0	0	50	37	0	1	0	2	
28	0	0	0	0	0	1	40	128	4	0	0	
29	0		0	0	0	0	78	33	1	0	0	
30	0		0	0	4	4	69	24	22	0	0	
31	0		0		0		6	6		0		
Total				74	95	434	446	743	245	599	170	28
										Annual Total=		2834
Daily Max	0	0	0	34	41	235	105	306	45	370	132	10
RainyDay				5	5	10	18	22	14	12	6	6

FIGURES

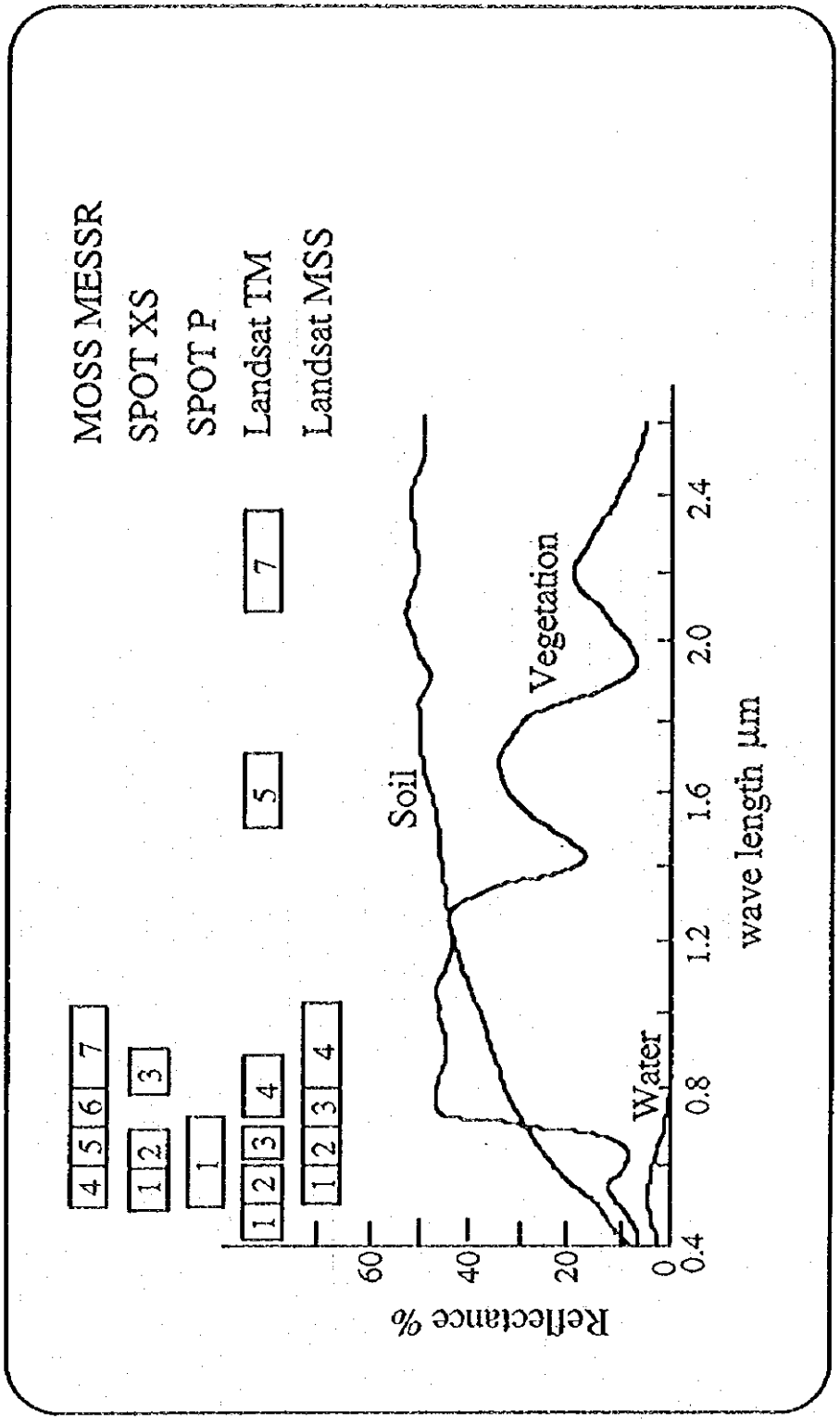

Figure Q.1 **Spectral response patterns of typical land cover classes**

THE GOVERNMENT OF THE PHILIPPINES
THE DEPARTMENT OF PUBLIC WORKS AND HIGHWAYS
THE STUDY ON FLOOD AND MUDFLOW CONTROL FOR SACOBIA-BAMBAN/ABACAN RIVER DRAINING FROM MT.PINATUBO
JAPAN INTERNATIONAL COOPERATION AGENCY

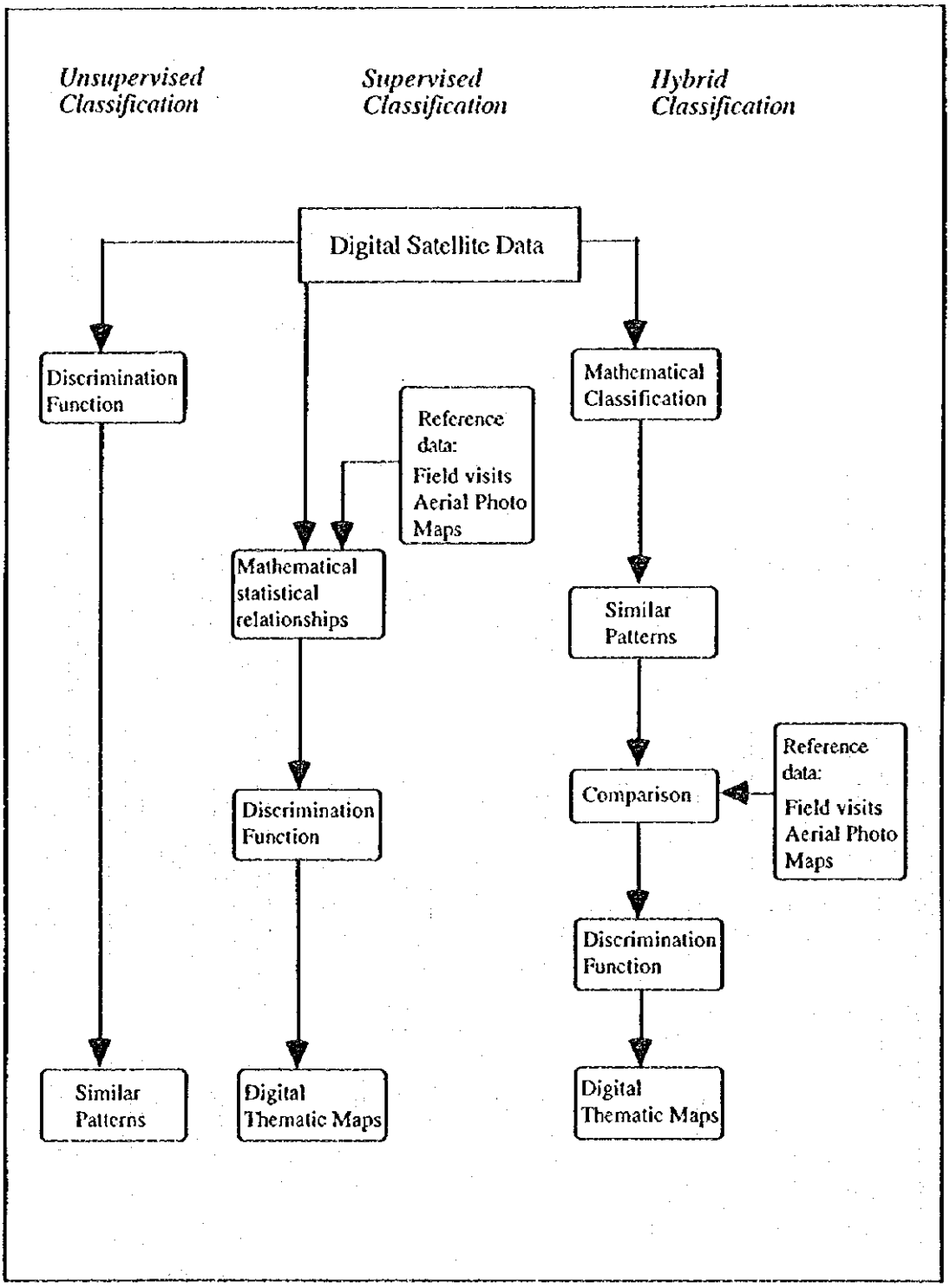

Figure Q.2 General procedure of digital classification of remotely sensed data

THE GOVERNMENT OF THE PHILIPPINES
THE DEPARTMENT OF PUBLIC WORKS AND HIGHWAYS
THE STUDY ON FLOOD AND MUDFLOW CONTROL FOR SACOBIA-BAMBAN/ABACAN RIVER DRAINING FROM MT.PINATUBO
JAPAN INTERNATIONAL COOPERATION AGENCY

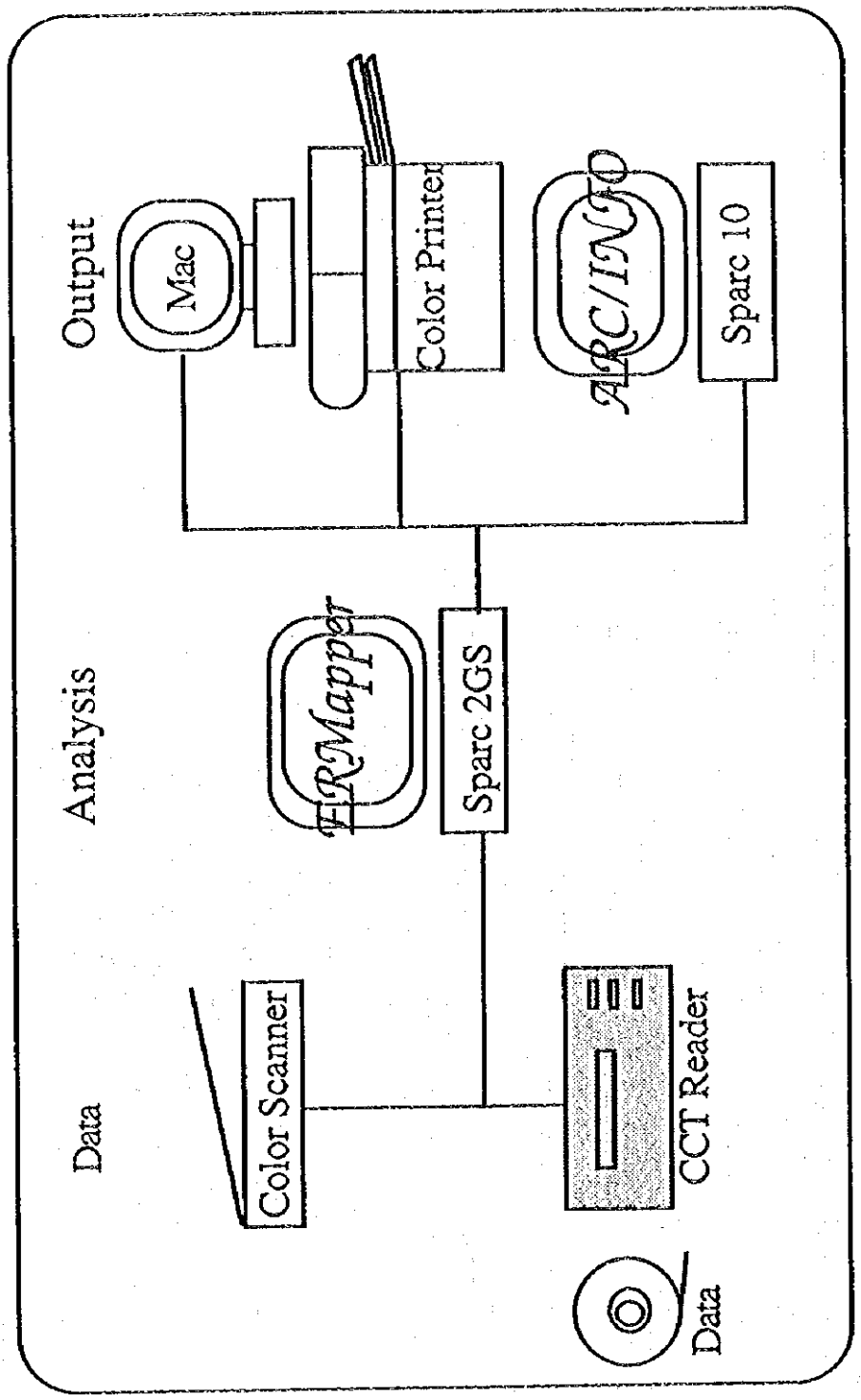

Figure Q.3 **Hardware and software configuration used for analysis**

THE GOVERNMENT OF THE PHILIPPINES THE DEPARTMENT OF PUBLIC WORKS AND HIGHWAYS
THE STUDY ON FLOOD AND MUDFLOW CONTROL FOR SACOBIA-BAMBAN/ABACAN RIVER DRAINING FROM MT.PINATUBO
JAPAN INTERNATIONAL COOPERATION AGENCY

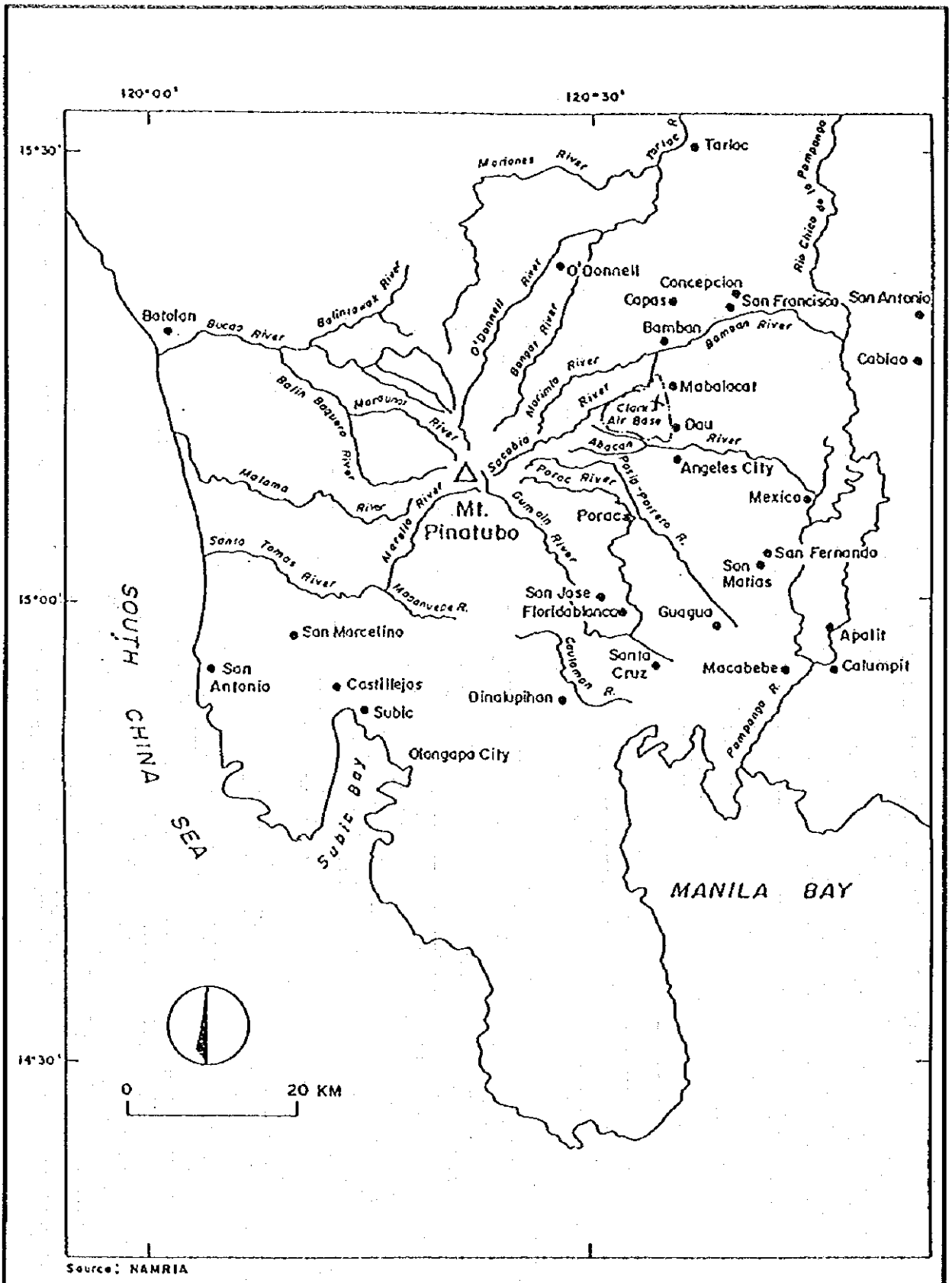

Figure Q.4 **Location of the study area and the major river network**

THE GOVERNMENT OF THE PHILIPPINES
THE DEPARTMENT OF PUBLIC WORKS AND HIGHWAYS
THE STUDY ON FLOOD AND MUDFLOW CONTROL FOR SACOBIA-BAMBAN/ABACAN RIVER DRAINING FROM MT.PINATUBO
JAPAN INTERNATIONAL COOPERATION AGENCY

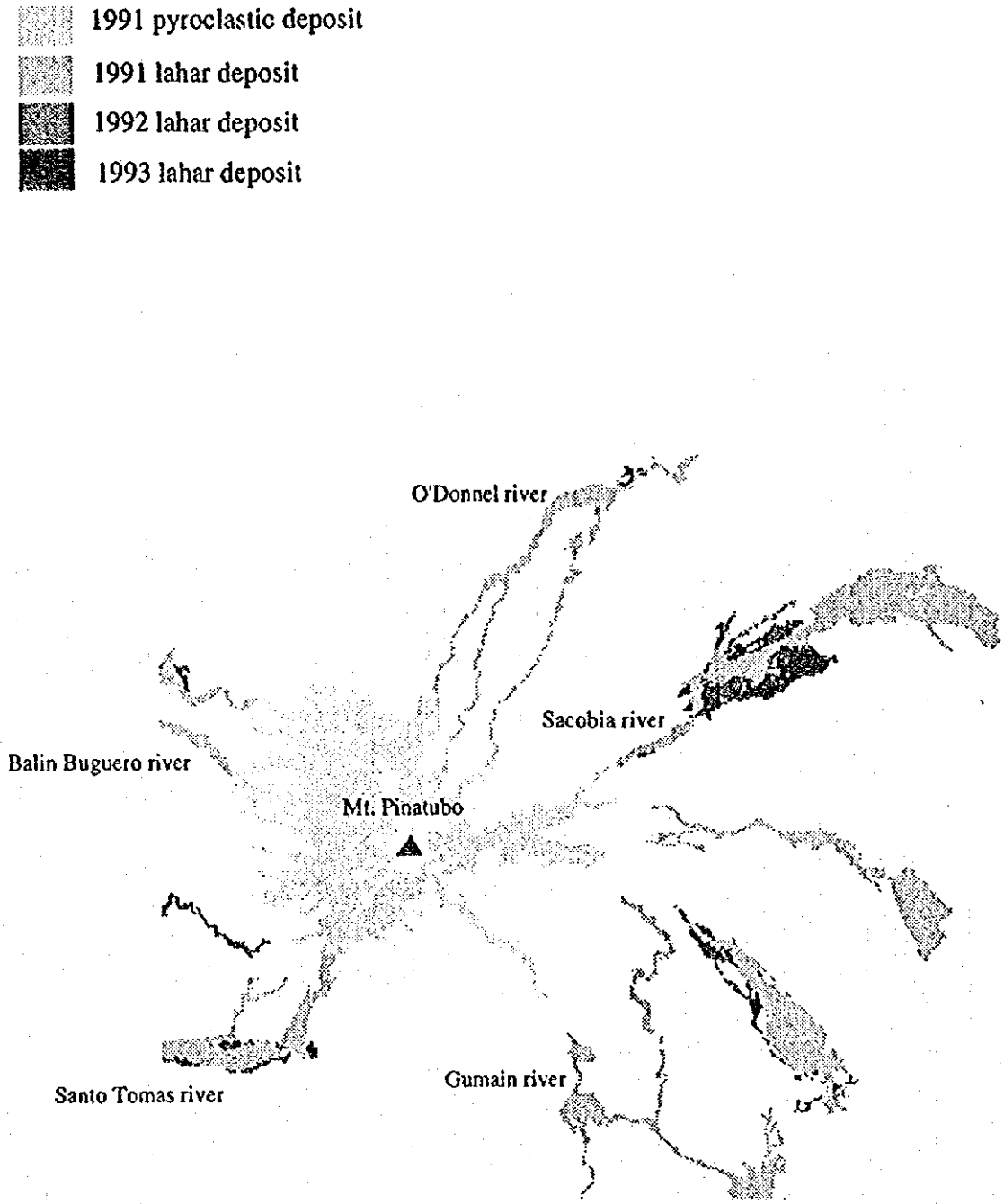

Figure Q.5 Pyroclastic and lahar estimates by DPWH

THE GOVERNMENT OF THE PHILIPPINES
THE DEPARTMENT OF PUBLIC WORKS AND HIGHWAYS
THE STUDY ON FLOOD AND MUDFLOW CONTROL FOR SACOBIA-BAMBAN/ABACAN RIVER DRAINING FROM MT.PINATUBO
JAPAN INTERNATIONAL COOPERATION AGENCY

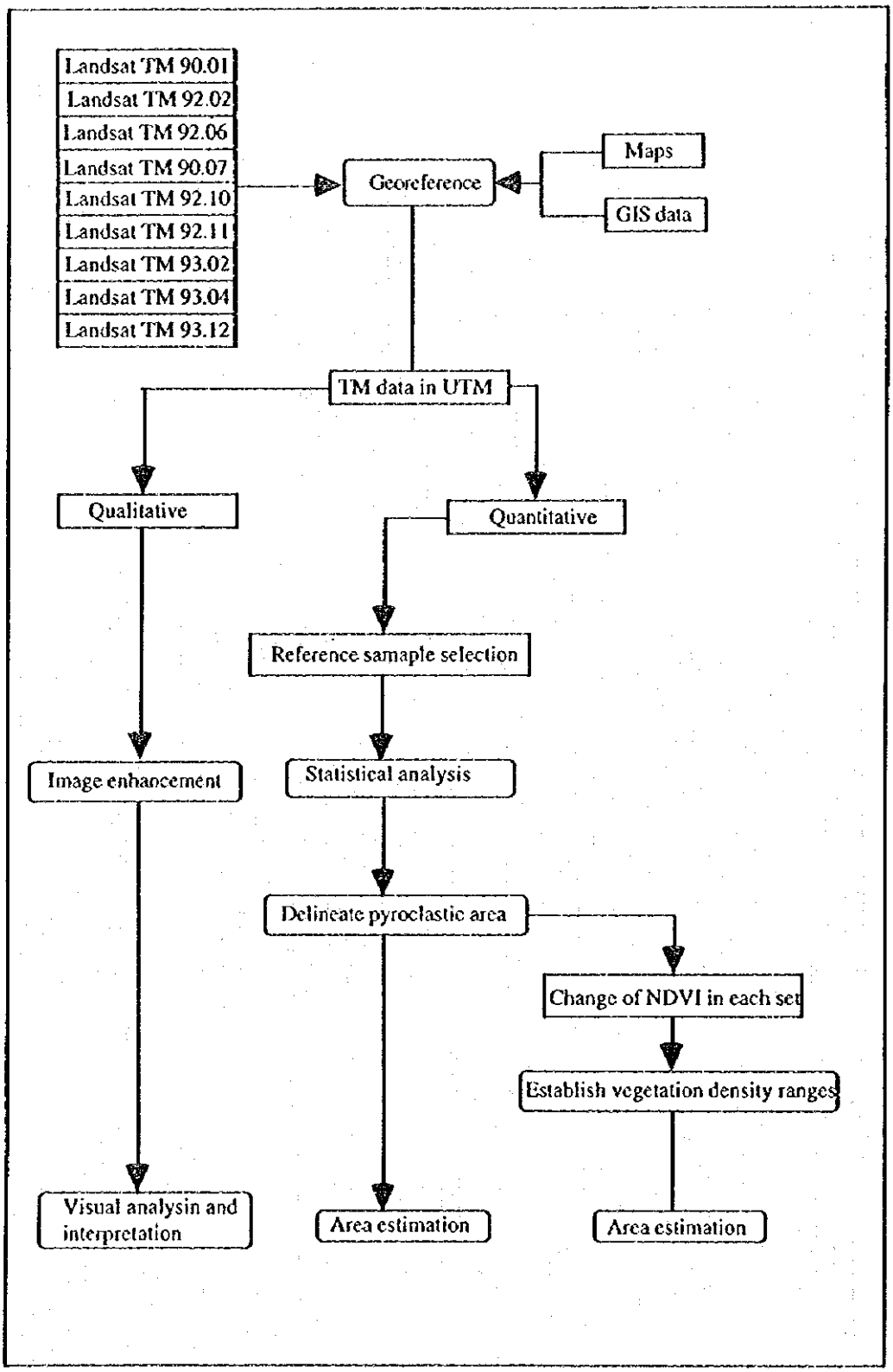

Figure Q.6 Criteria of satellite data analysis for the study

THE GOVERNMENT OF THE PHILIPPINES
THE DEPARTMENT OF PUBLIC WORKS AND HIGHWAYS
THE STUDY ON FLOOD AND MUDFLOW CONTROL FOR SACOBIA-BAMBAN/ABACAN RIVER DRAINING FROM MT.PINATUBO
JAPAN INTERNATIONAL COOPERATION AGENCY

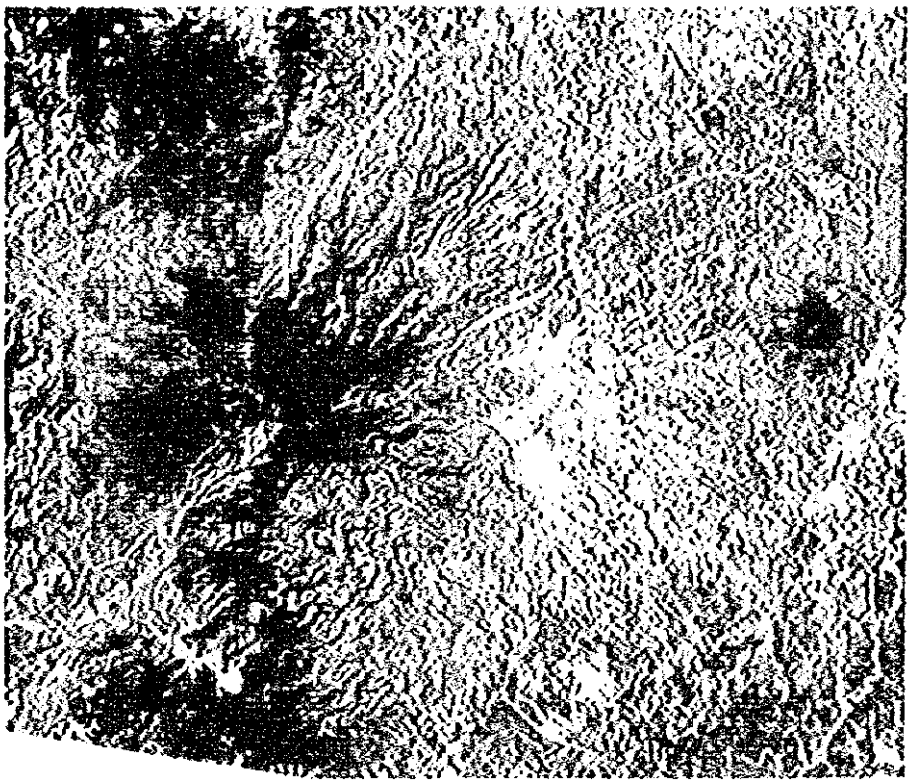

Figure Q.7 Natural color composite of 1990 January TM data

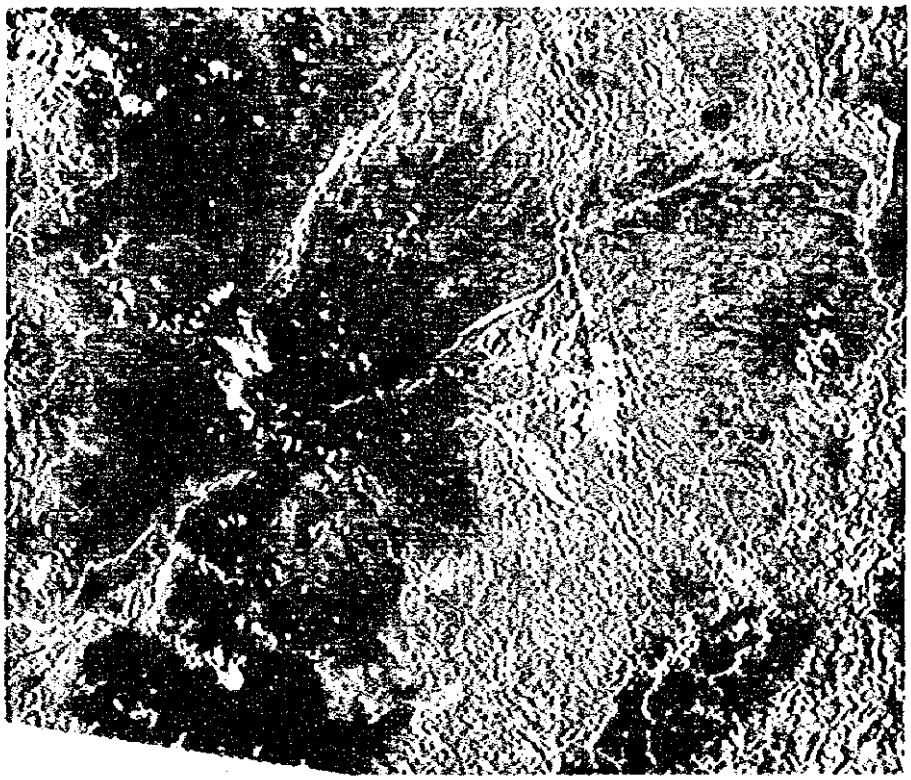

Figure Q.8 Natural color composite of 1990 July TM data

Figure Q.9 Natural color composite of 1992 February TM data

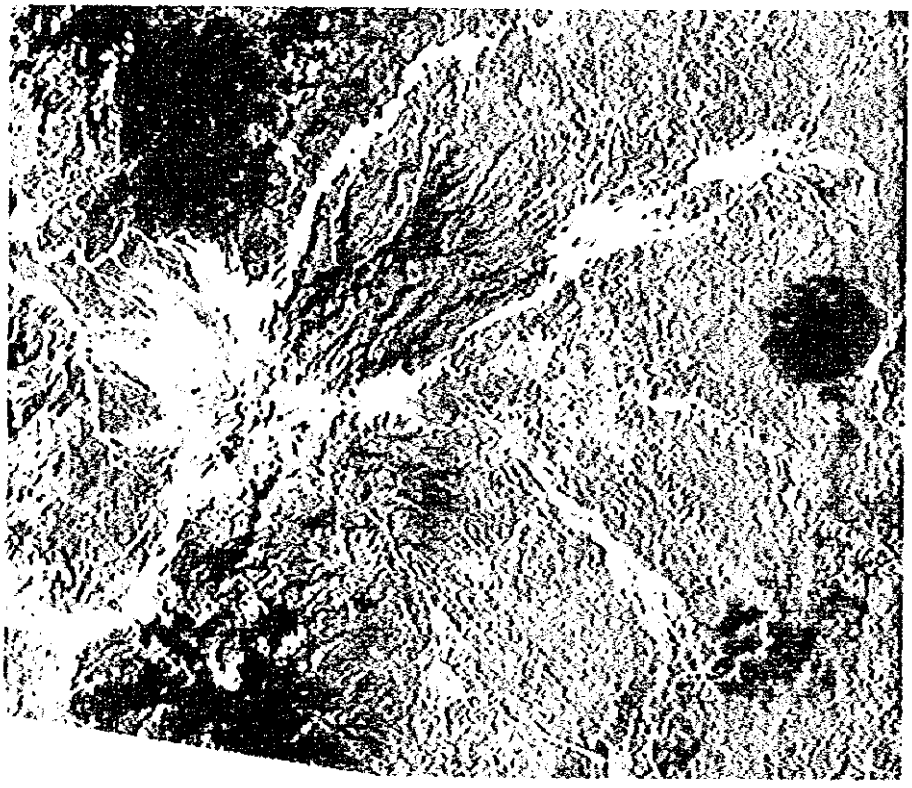

Figure Q.10 Natural color composite of 1992 November TM data

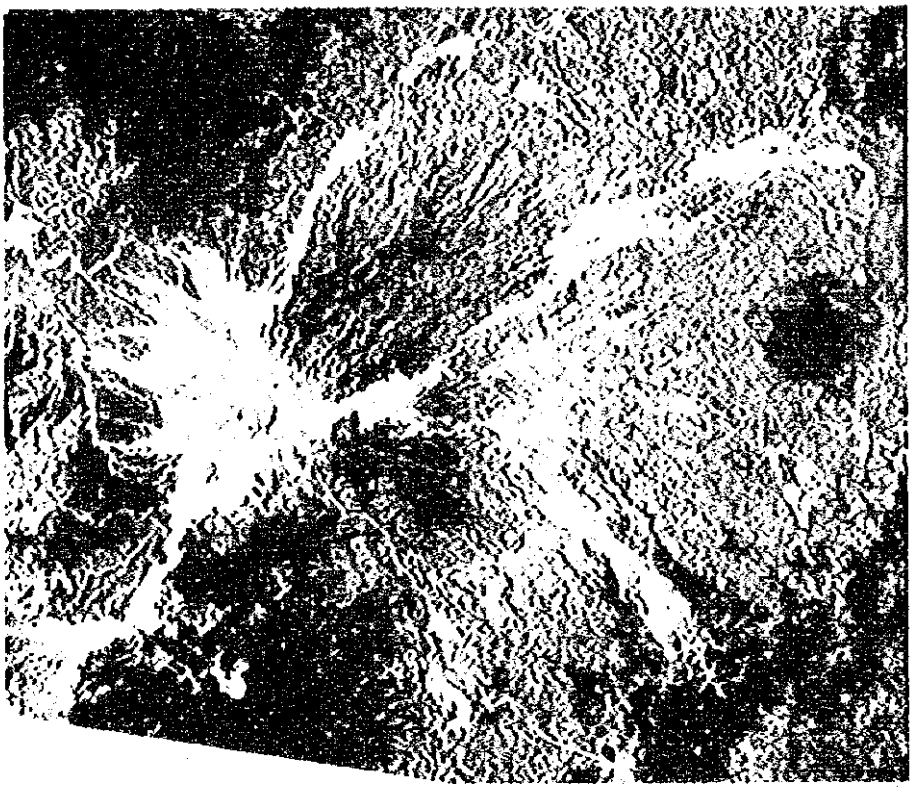

Figure Q.11 Natural color composite of 1993 April TM data

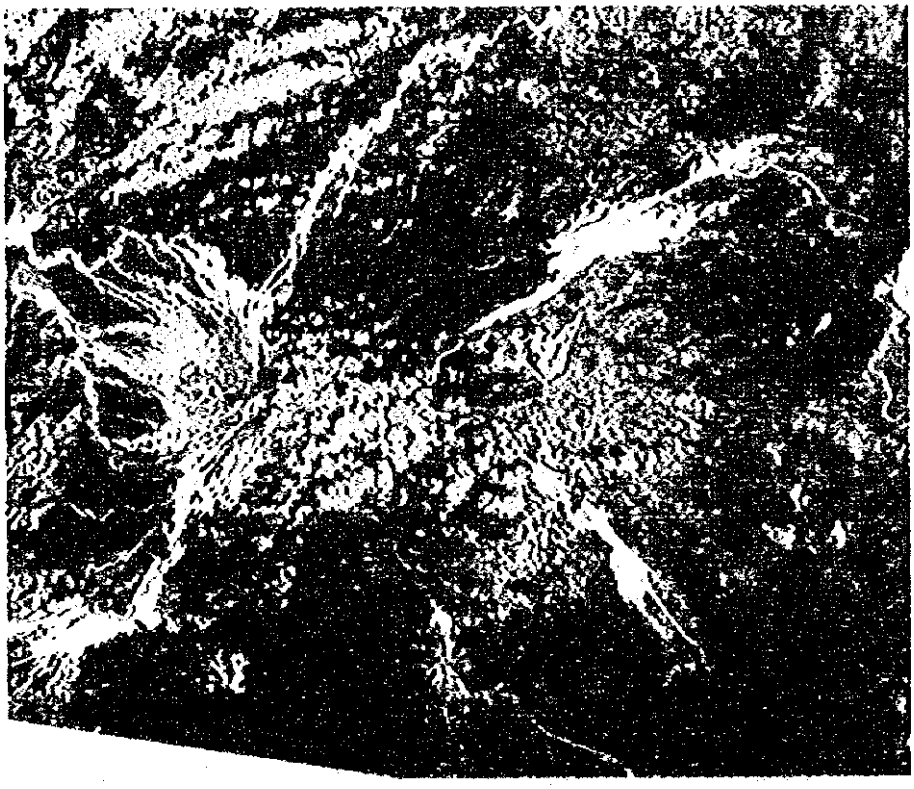

Figure Q.12 Natural color composite of 1993 December TM data

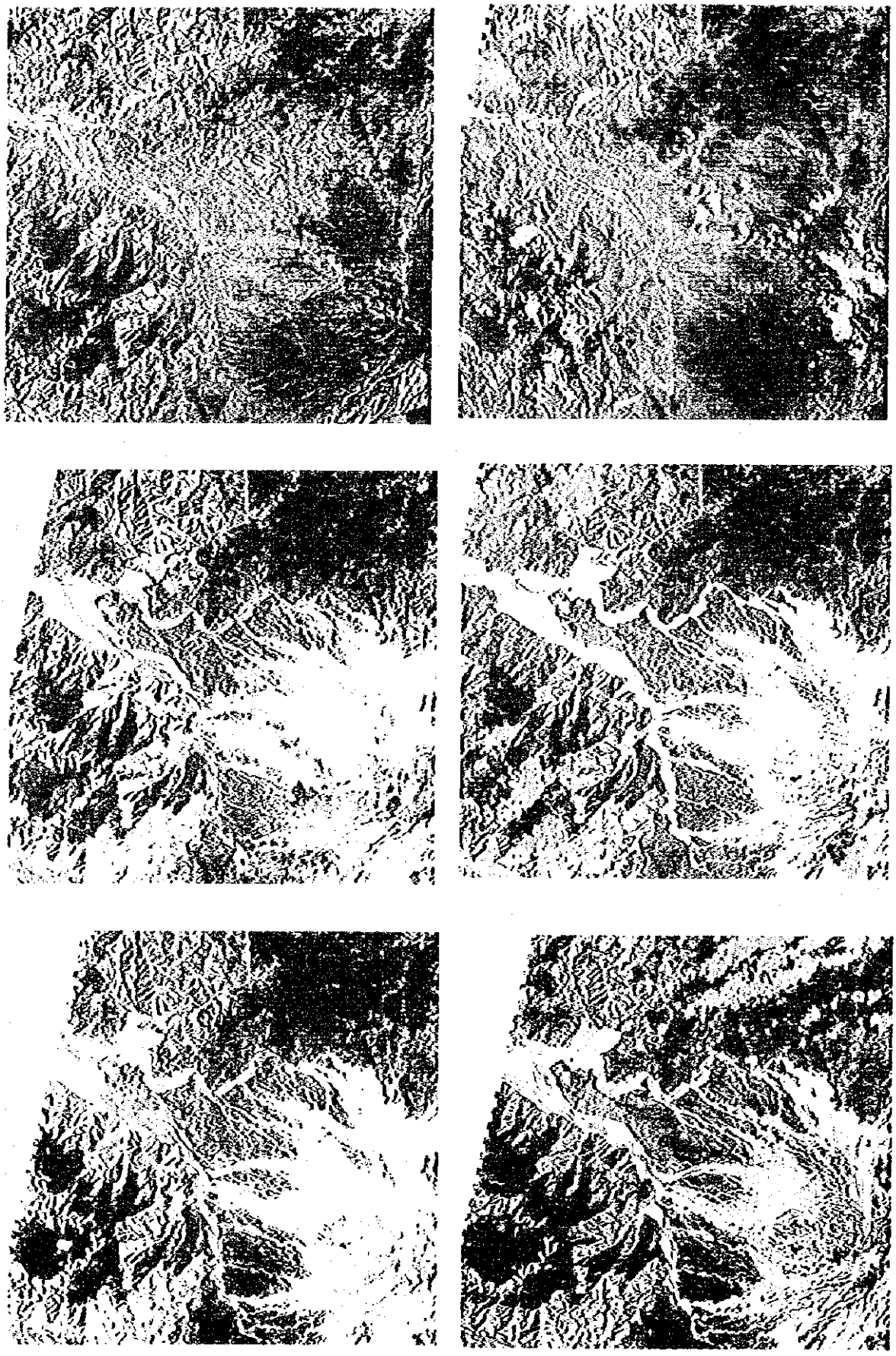

Figure Q.13 Natural color composite of North-West part of the study area

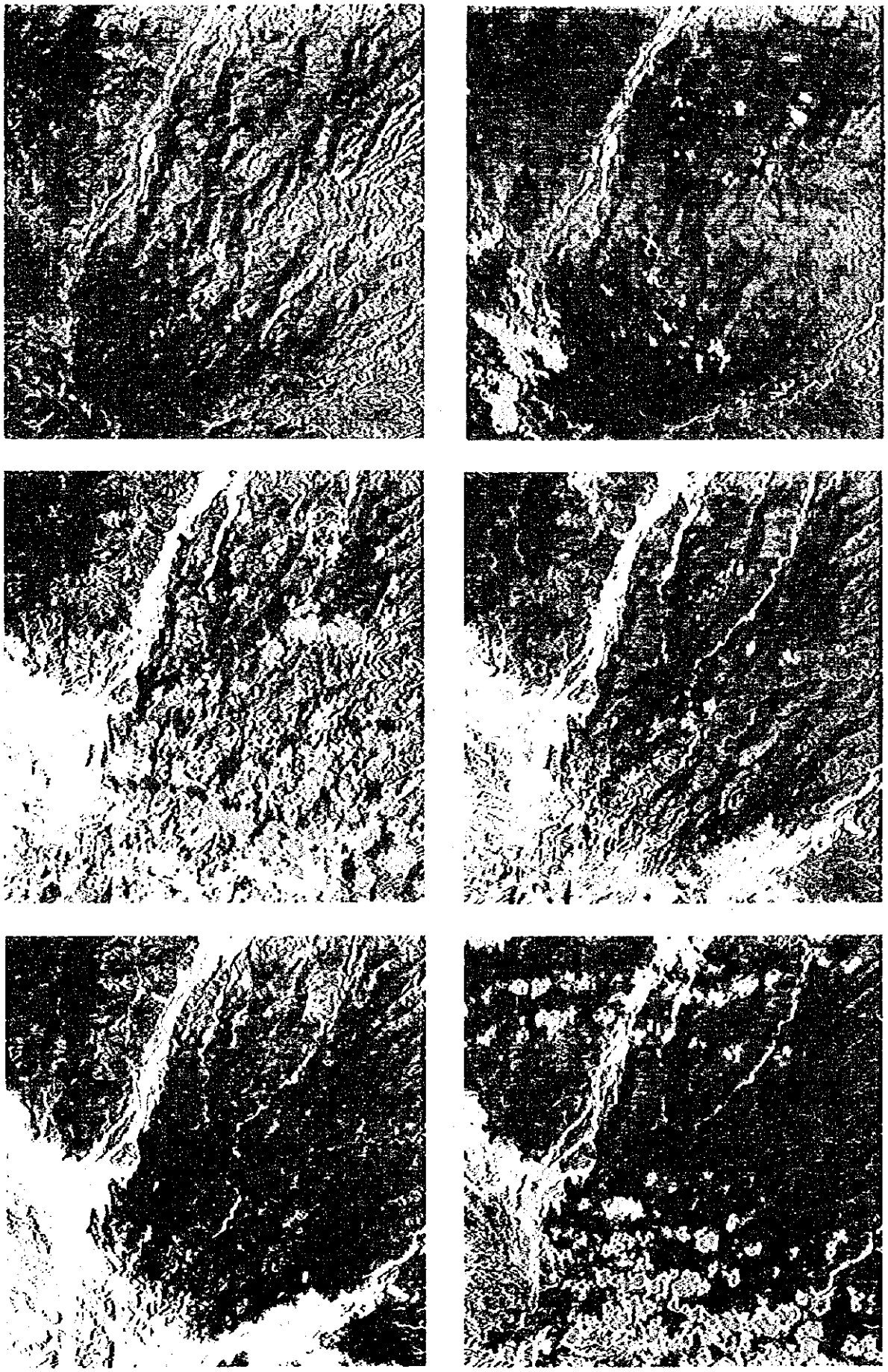

Figure Q.14 Natural color composite of North-East part of the study area

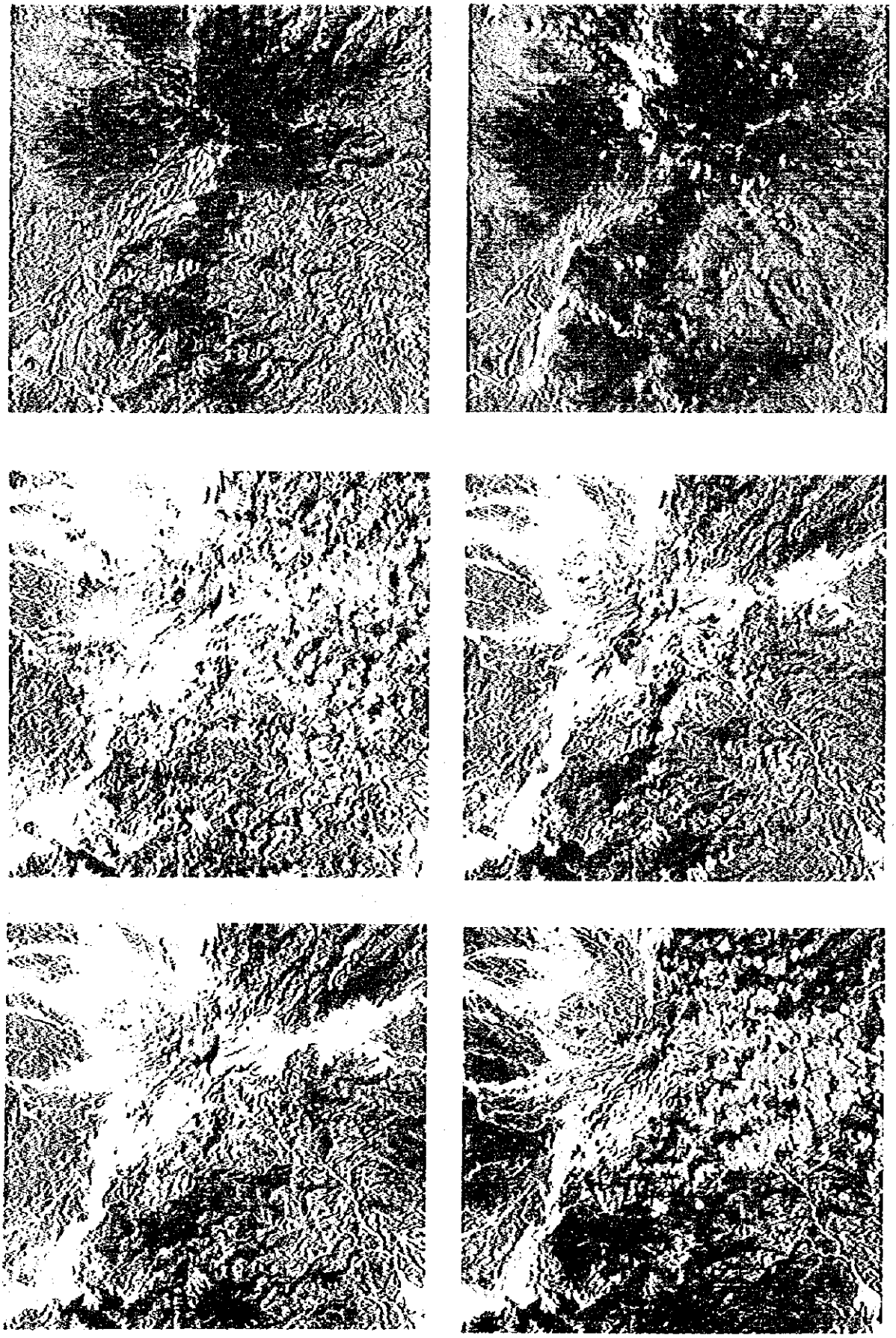

Figure Q.15 Natural color composite of South-East part of the study area

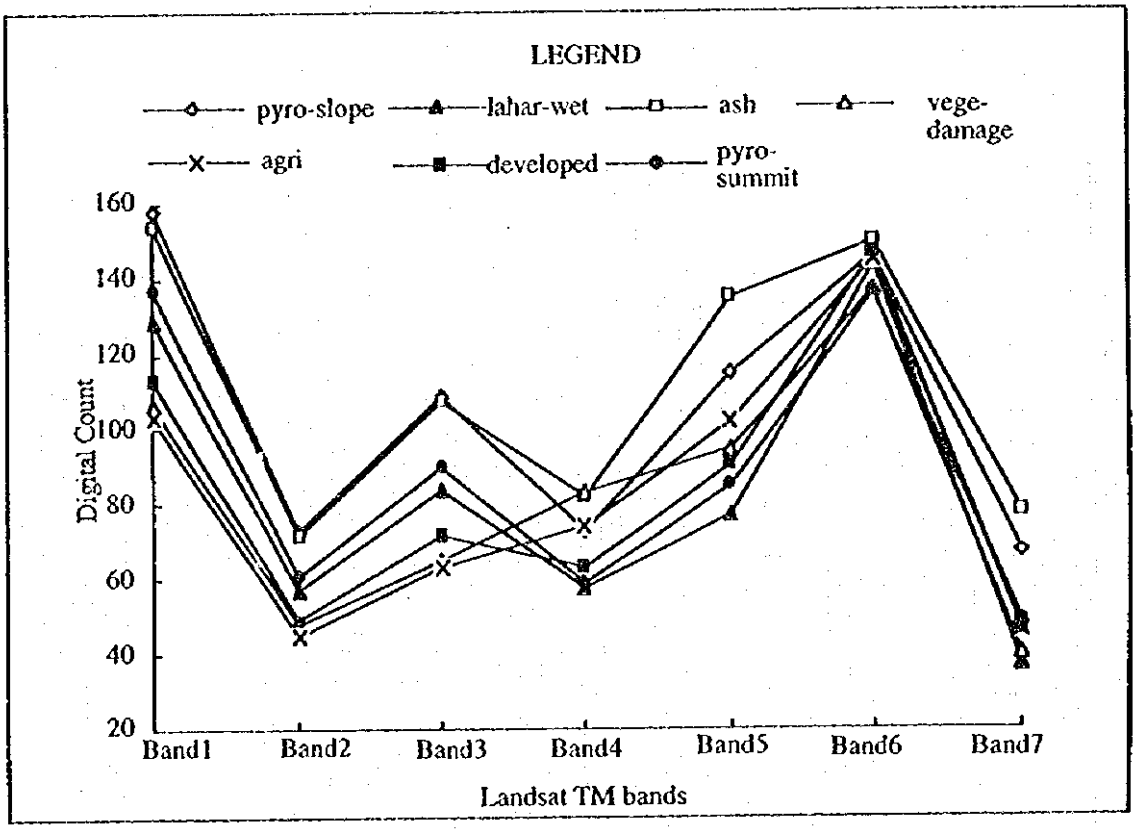

Figure Q.16 Spectral response patterns of Landsat TM data of 1992 February

THE GOVERNMENT OF THE PHILIPPINES
THE DEPARTMENT OF PUBLIC WORKS AND HIGHWAYS
THE STUDY ON FLOOD AND MUDFLOW CONTROL FOR SACOBIA-BAMBAN/ABACAN RIVER DRAINING FROM MT.PINATUBO
JAPAN INTERNATIONAL COOPERATION AGENCY

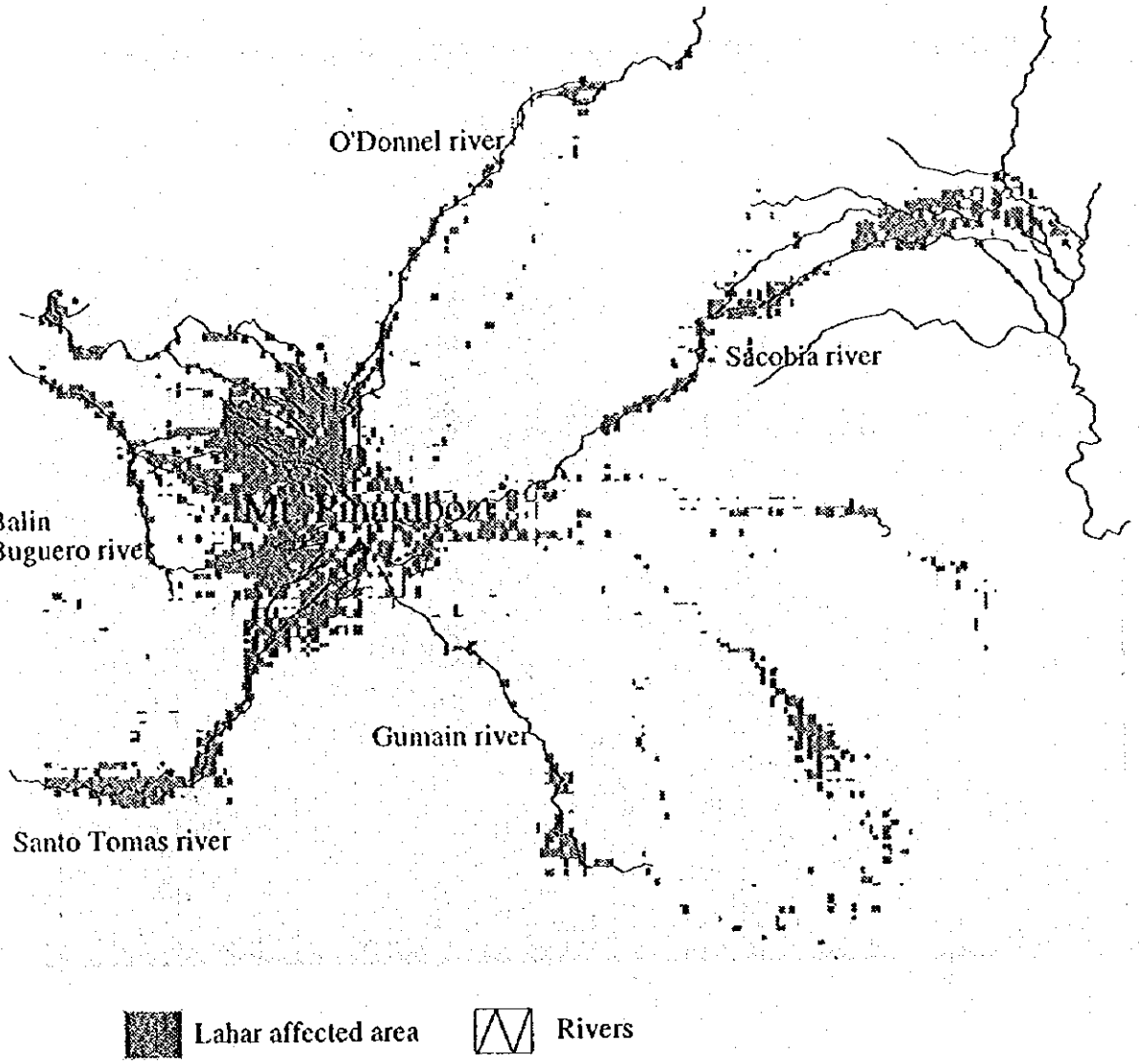

Figure Q.17 Estimation of pyroclastic and lahar extent by 1992 February TM data

THE GOVERNMENT OF THE PHILIPPINES
THE DEPARTMENT OF PUBLIC WORKS AND HIGHWAYS
THE STUDY ON FLOOD AND MUDFLOW CONTROL FOR SACOBIA-BAMBAN/ABACAN RIVER DRAINING FROM MT PINATUBO
JAPAN INTERNATIONAL COOPERATION AGENCY

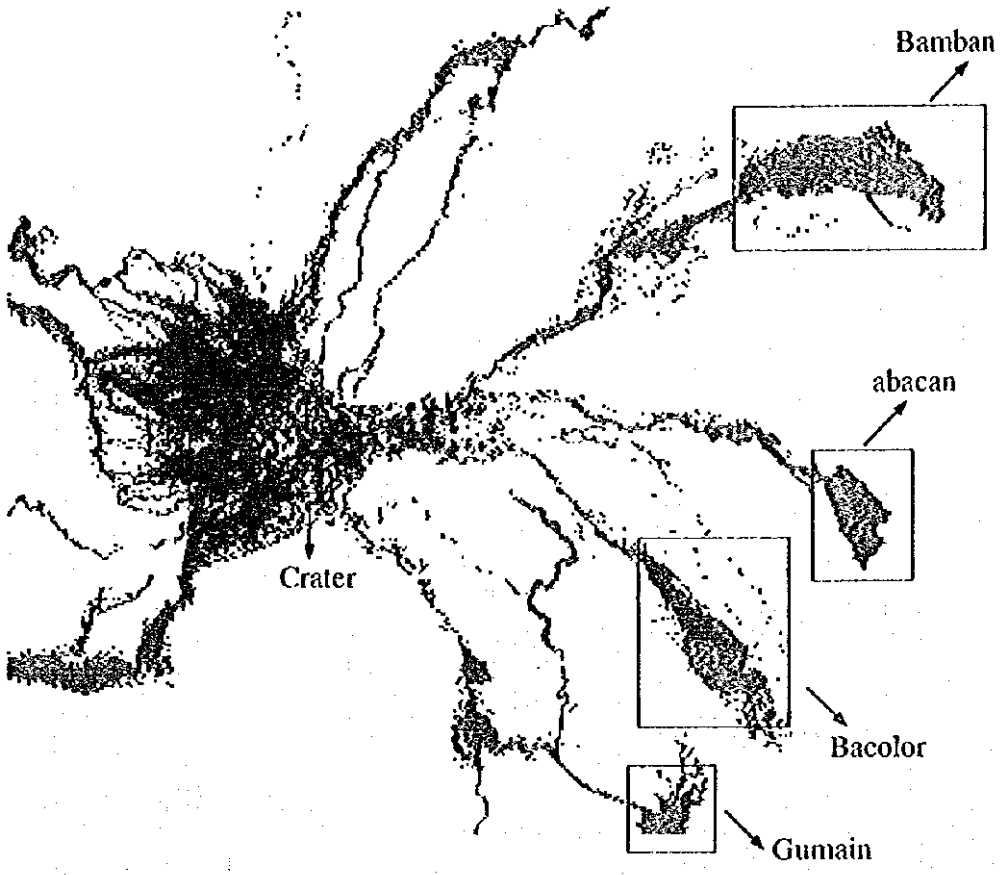

LEGEND

- DPWH pyroclastic - TM pyroclastic or lahar
- DPWH pyroclastic - TM un-damaged
- TM pyorocalstic or lahar - DPWH un-damaged
- DPWH lahar - TM pyroclastic or lahar
- DPWH lahar - TM un-damaged

Figure Q.18 Comparison of 1992 February TM data estimation of damaged area with DPWH surveys

THE GOVERNMENT OF THE PHILIPPINES
THE DEPARTMENT OF PUBLIC WORKS AND HIGHWAYS
THE STUDY ON FLOOD AND MUDFLOW CONTROL FOR SACOBIA-BAMBAN/ABACAN RIVER DRAINING FROM MT.PINATUBO
JAPAN INTERNATIONAL COOPERATION AGENCY

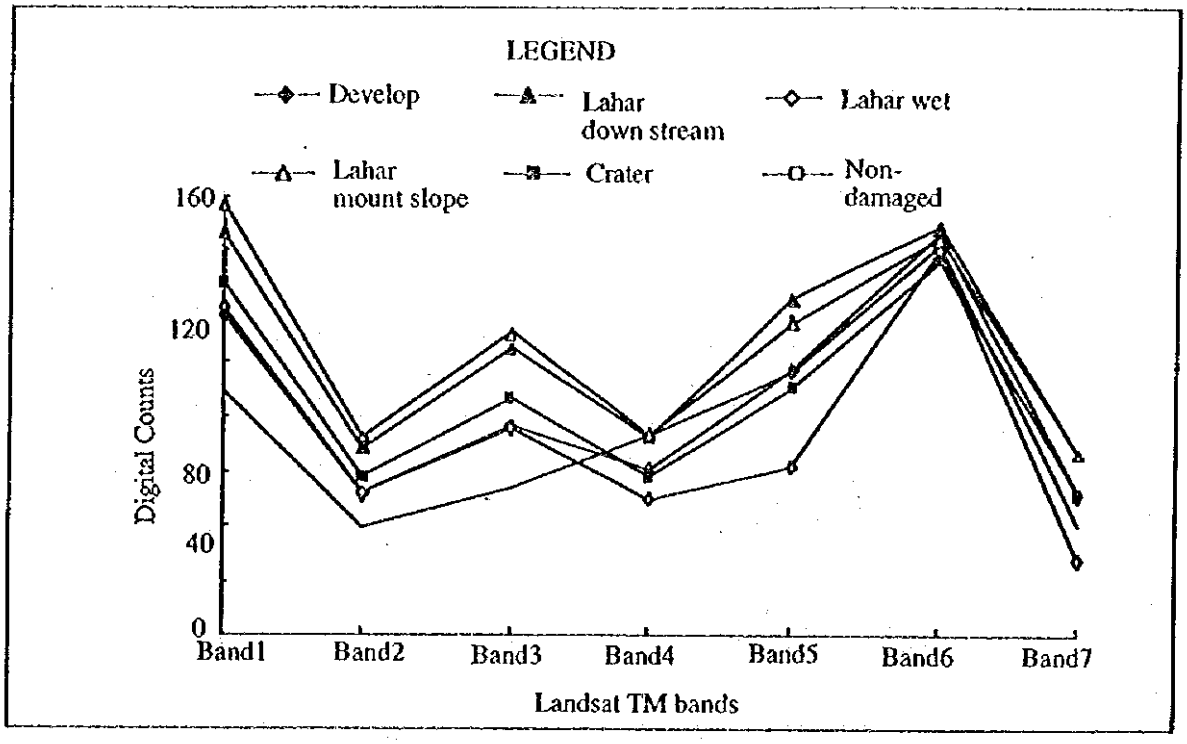

Figure Q.19 Spectral response patterns of Landsat TM data of 1993 February

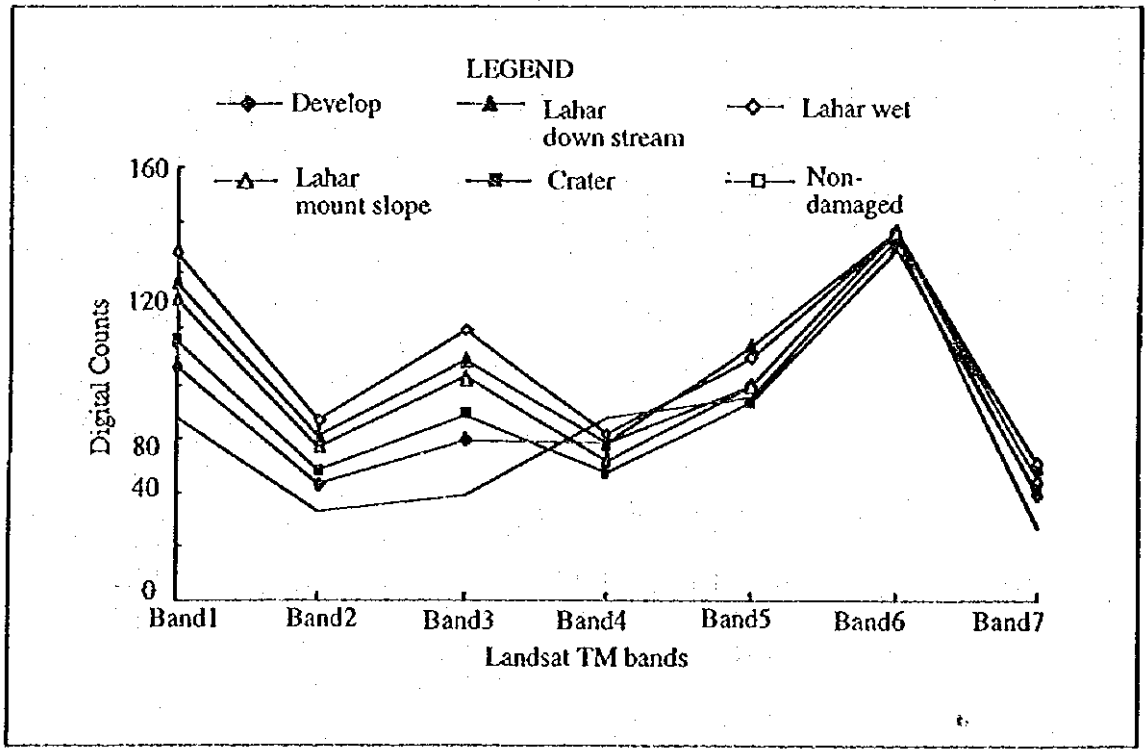

Figure Q.20 Spectral response patterns of Landsat TM data of 1993 December

THE GOVERNMENT OF THE PHILIPPINES
THE DEPARTMENT OF PUBLIC WORKS AND HIGHWAYS
THE STUDY ON FLOOD AND MUDFLOW CONTROL FOR SACOBIA-BAMBAN/ABACAN RIVER DRAINING FROM MT.PINATUBO
JAPAN INTERNATIONAL COOPERATION AGENCY

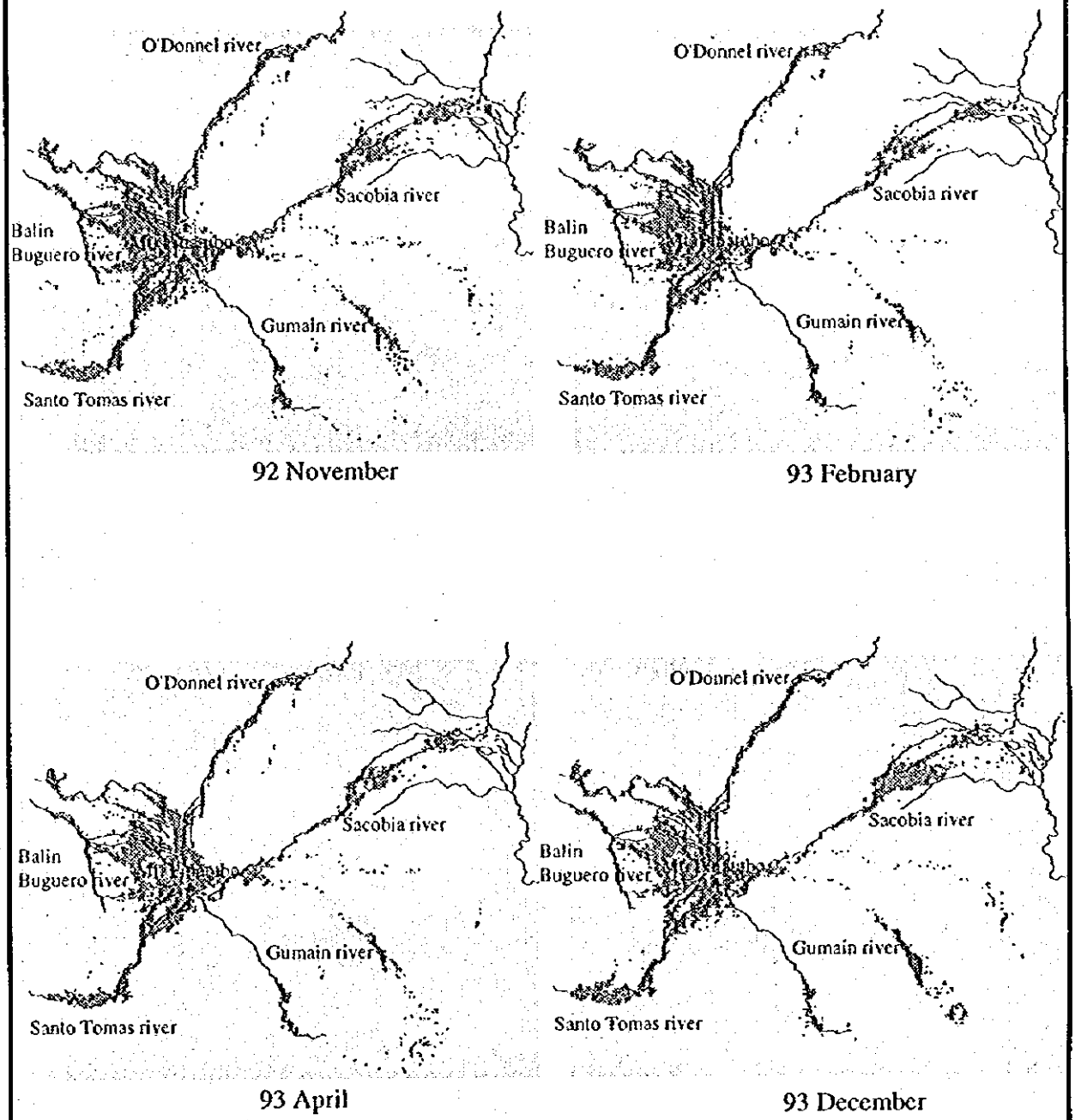

Figure Q.21 Estimation of pyroclastic and lahar extent for multitemporal TM datasets

THE GOVERNMENT OF THE PHILIPPINES
THE DEPARTMENT OF PUBLIC WORKS AND HIGHWAYS
THE STUDY ON FLOOD AND MUDFLOW CONTROL FOR SACOBIA-BAMBAN/ABACAN RIVER DRAINING FROM MT.PINATUBO
JAPAN INTERNATIONAL COOPERATION AGENCY

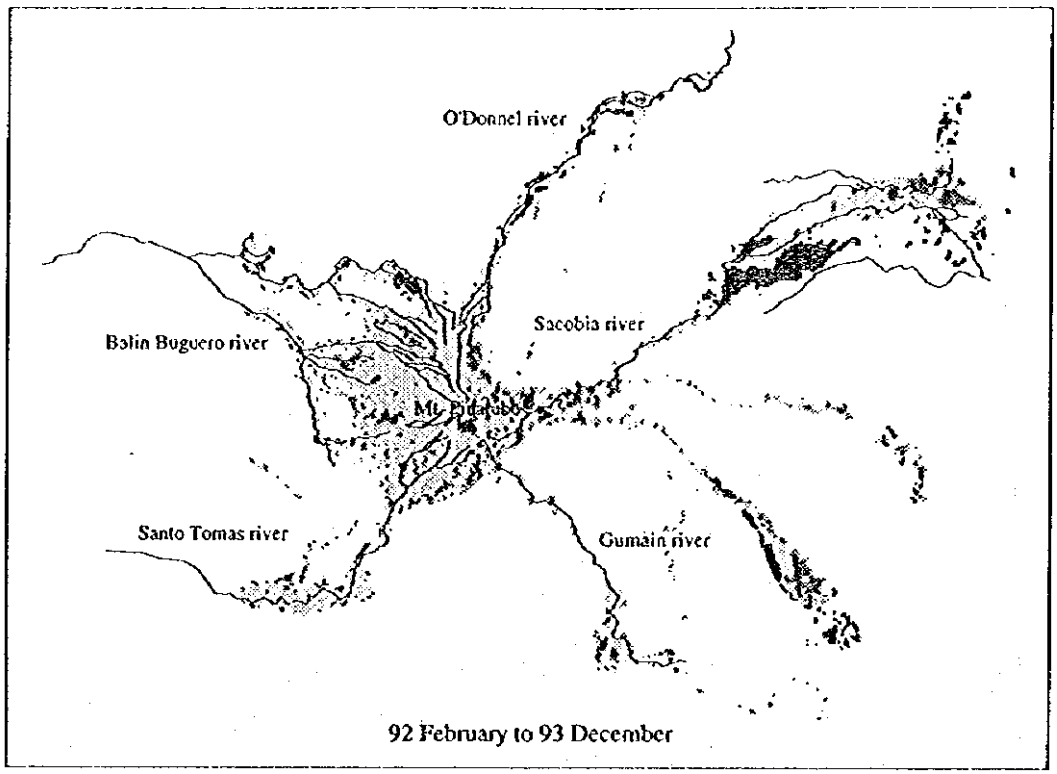

LEGEND

No change | Increase | Decrease | River

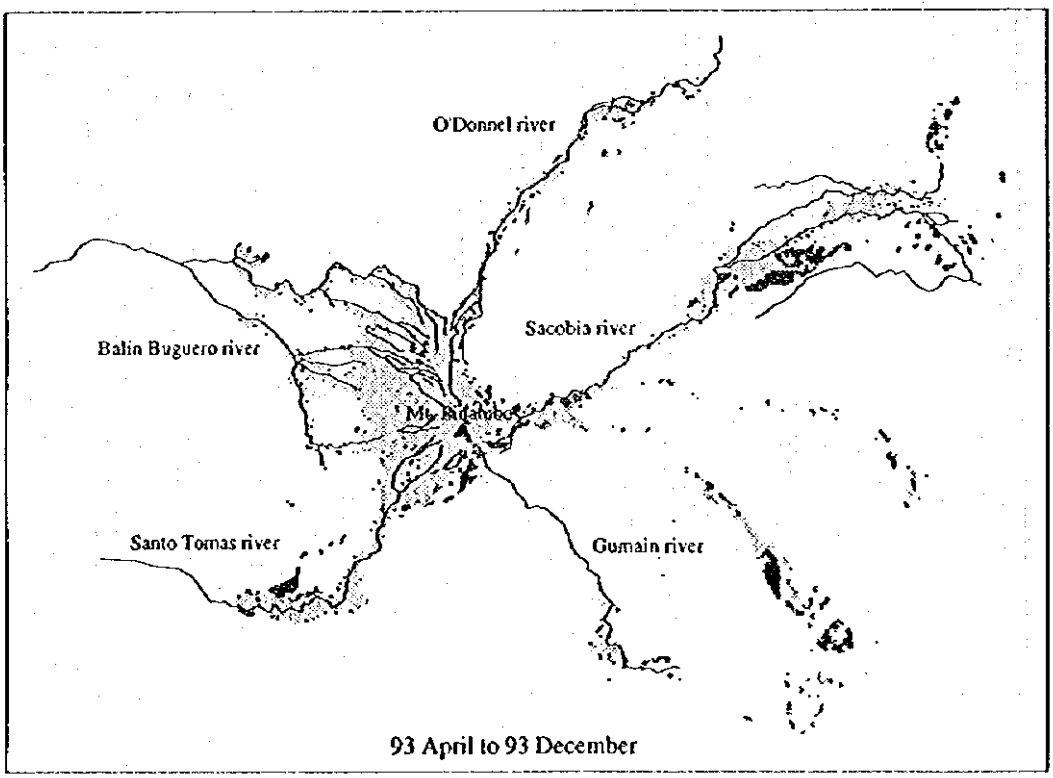

Figure Q.22.1 Changes between damaged extents as observed by TM data classification

THE GOVERNMENT OF THE PHILIPPINES
THE DEPARTMENT OF PUBLIC WORKS AND HIGHWAYS
THE STUDY ON FLOOD AND MUDFLOW CONTROL FOR SACOBIA-BAMBAN/ABACAN RIVER DRAINING FROM MT.PINATUBO
JAPAN INTERNATIONAL COOPERATION AGENCY

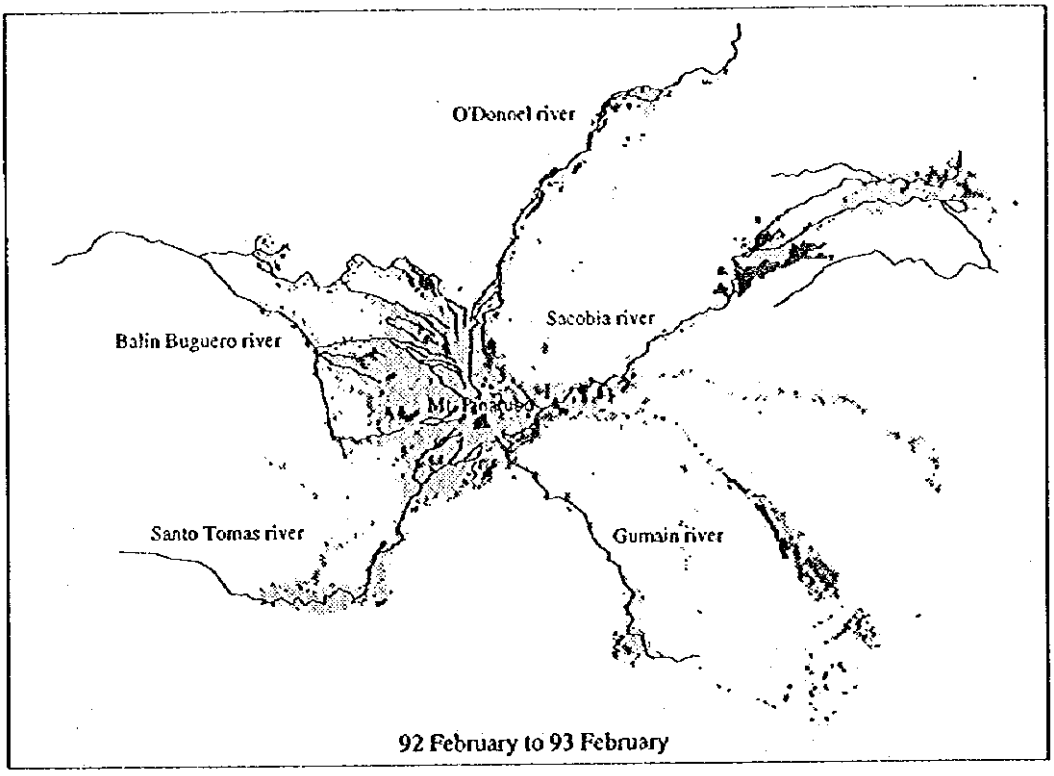

LEGEND

No change | Increase | Decrease | River

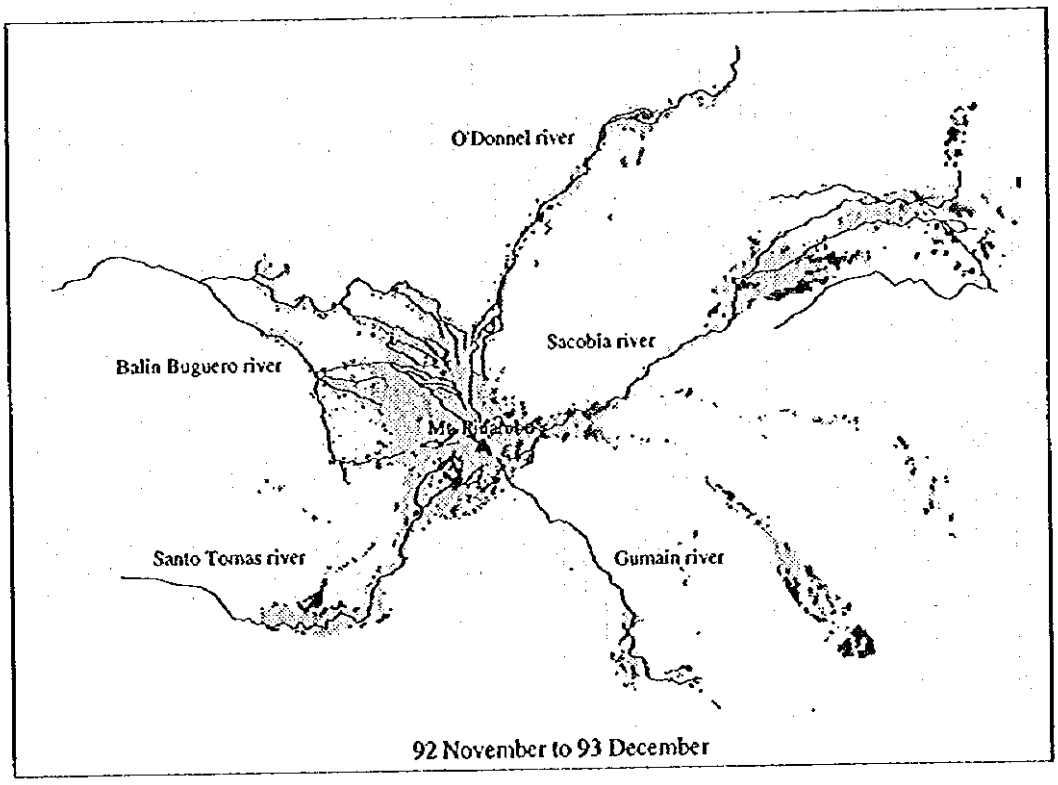

Figure Q.22.2 Changes between damaged extents as observed by TM data classification

THE GOVERNMENT OF THE PHILIPPINES
THE DEPARTMENT OF PUBLIC WORKS AND HIGHWAYS
THE STUDY ON FLOOD AND MUDFLOW CONTROL FOR SACOBIA-BAMBAN/ABACAN RIVER DRAINING FROM MT.PINATUBO
JAPAN INTERNATIONAL COOPERATION AGENCY

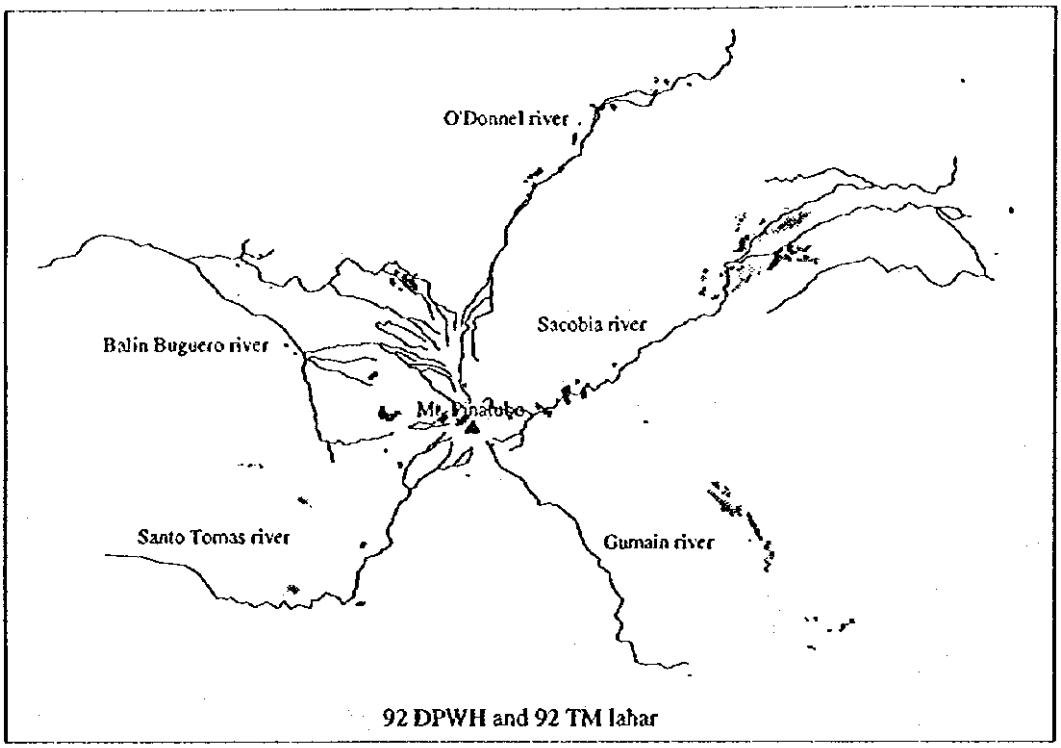

92 DPWH and 92 TM lahar

LEGEND

DPWH lahar - TM lahar | TMlahar - DPWH undamaged | DPWH lahar - TM undamaged

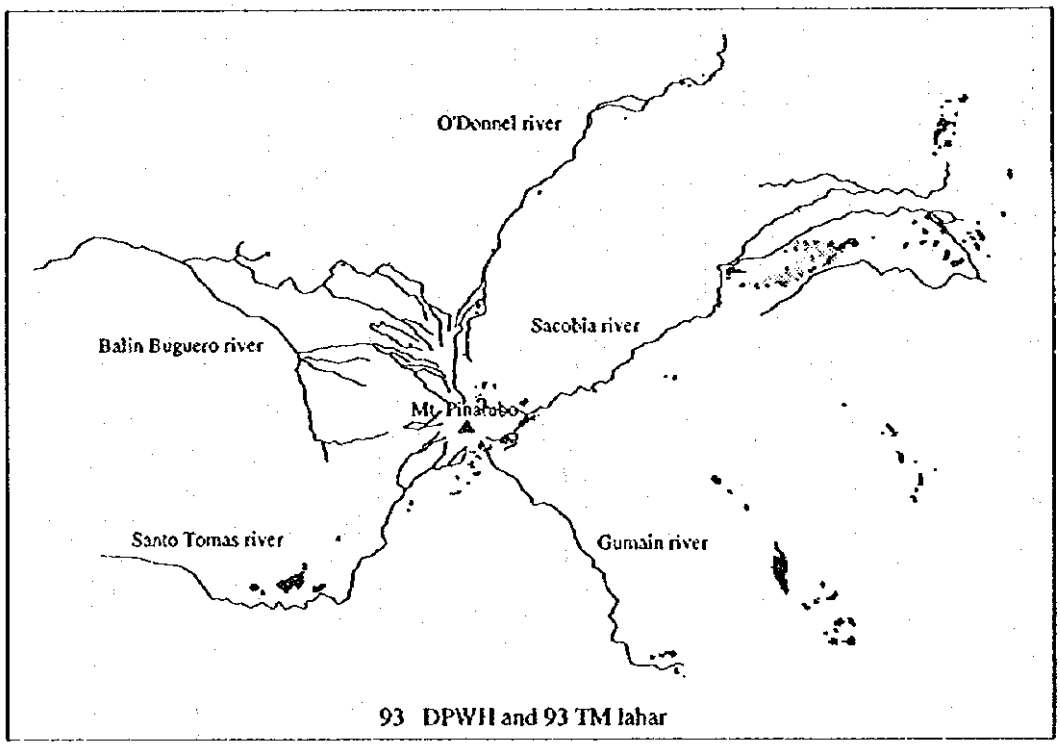

93 DPWH and 93 TM lahar

Figure Q.23 Comparison of DPWH and TM data estimation for 1992 and 1993

THE GOVERNMENT OF THE PHILIPPINES
THE DEPARTMENT OF PUBLIC WORKS AND HIGHWAYS
THE STUDY ON FLOOD AND MUDFLOW CONTROL FOR SACOBIA-BAMBAN/ABACAN RIVER DRAINING FROM MT.PINATUBO
JAPAN INTERNATIONAL COOPERATION AGENCY

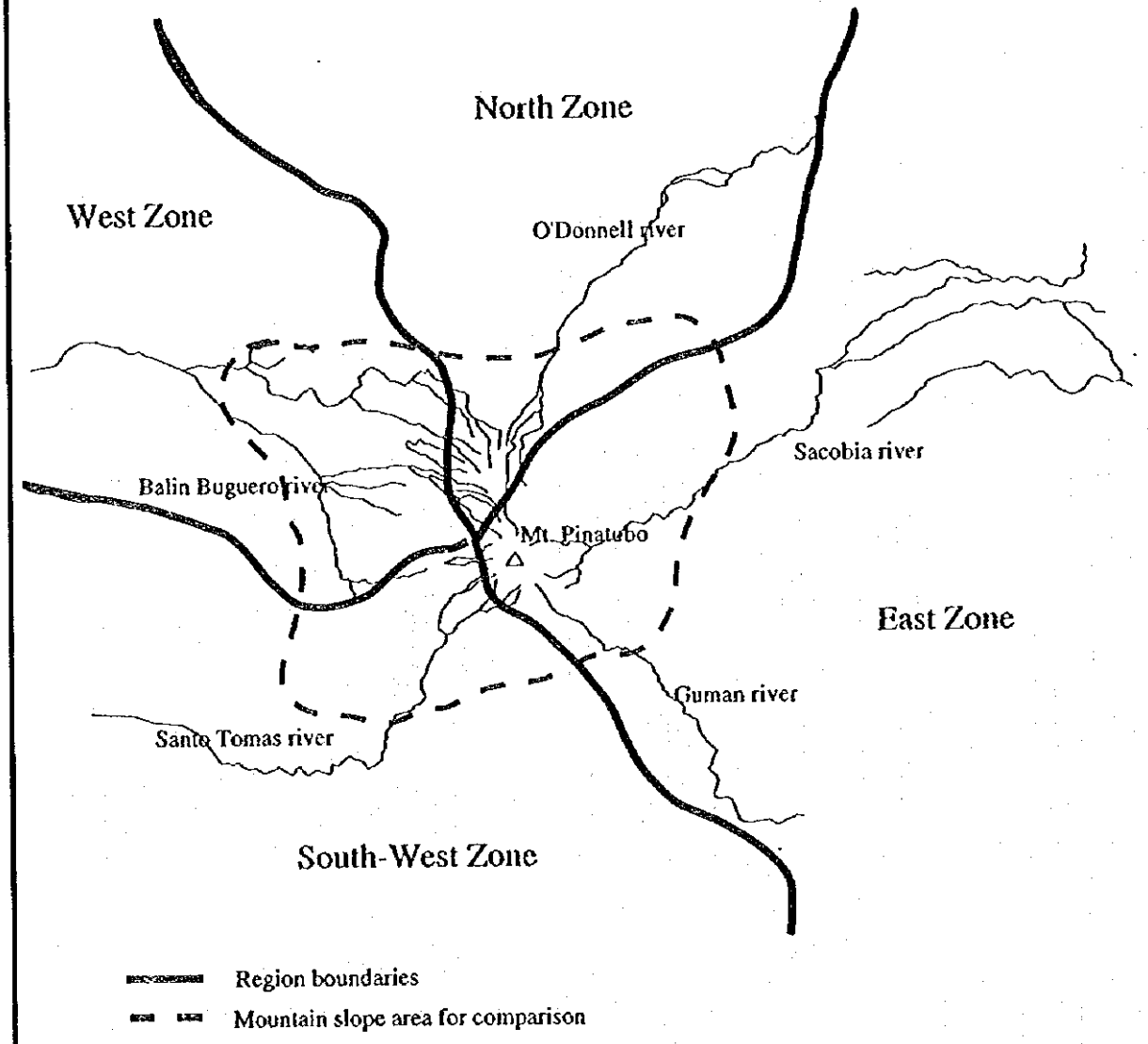

Figure Q.24 Defined zones for detailed investigation of damage and changes

THE GOVERNMENT OF THE PHILIPPINES
THE DEPARTMENT OF PUBLIC WORKS AND HIGHWAYS
THE STUDY ON FLOOD AND MUDFLOW CONTROL FOR SACOBIA-BAMBAN/ABACAN RIVER DRAINING FROM MT.PINATUBO
JAPAN INTERNATIONAL COOPERATION AGENCY

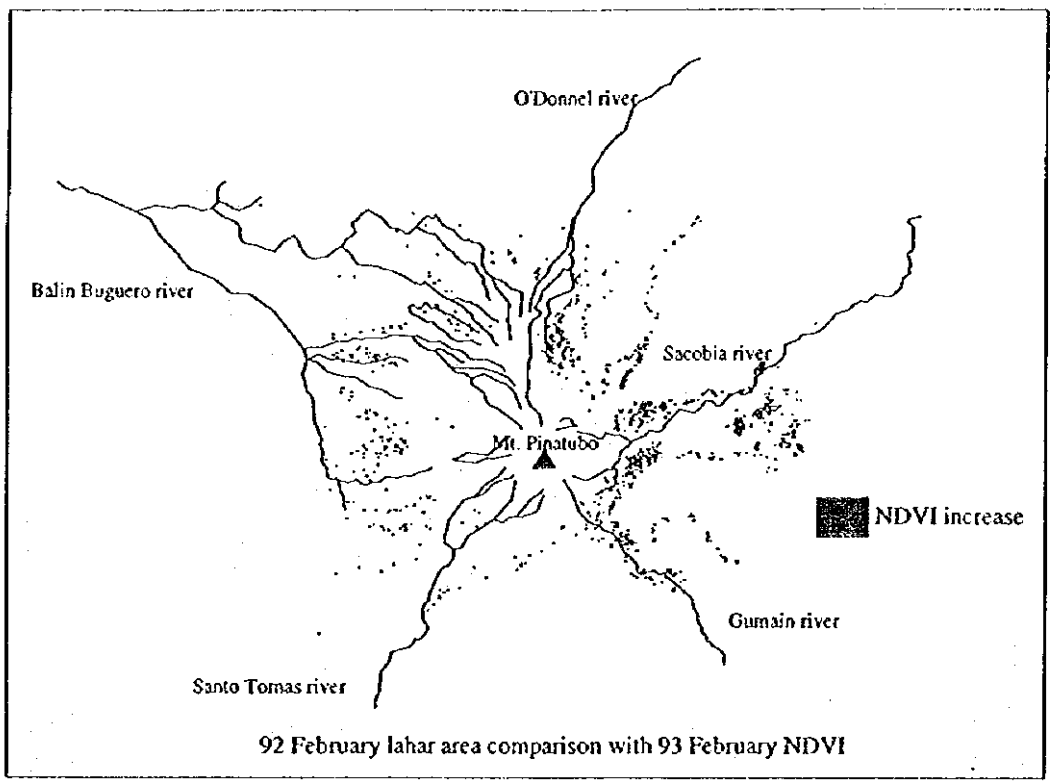

92 February lahar area comparison with 93 February NDVI

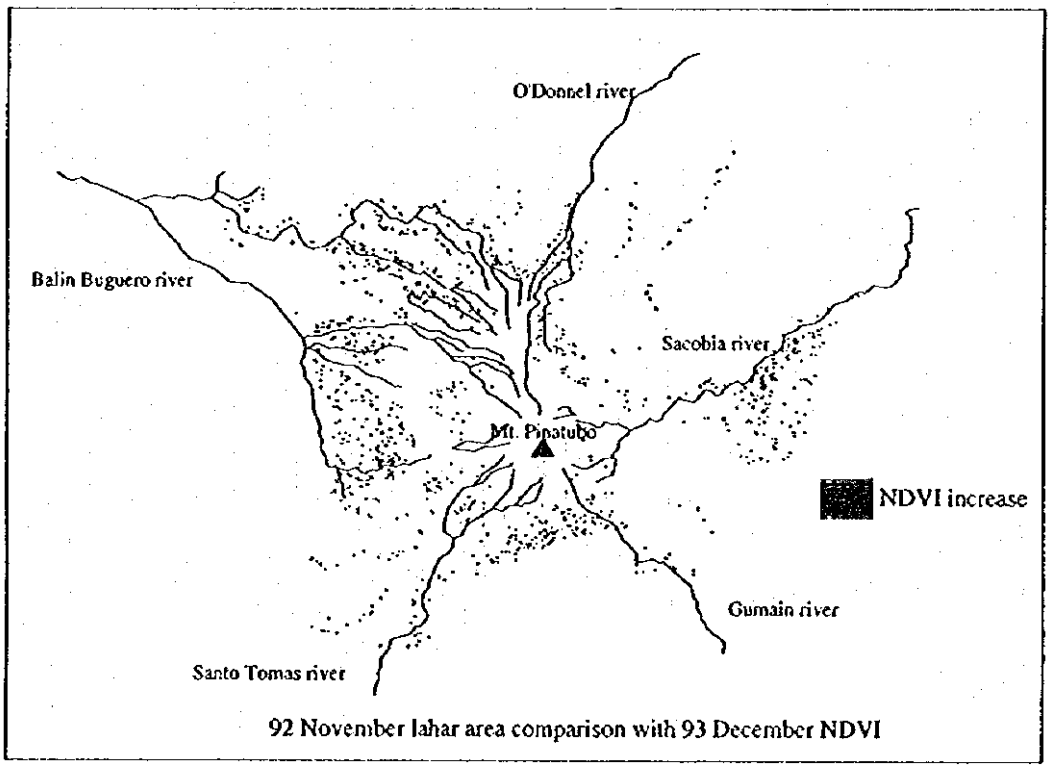

92 November lahar area comparison with 93 December NDVI

Figure Q.25 Estimation of NDVI changes during 1992 February to 1993 February and 1992 November to 19

THE GOVERNMENT OF THE PHILIPPINES
THE DEPARTMENT OF PUBLIC WORKS AND HIGHWAYS
THE STUDY ON FLOOD AND MUDFLOW CONTROL FOR SACOBIA-BAMBAN/ABACAN RIVER DRAINING FROM MT.PINATUBO
JAPAN INTERNATIONAL COOPERATION AGENCY

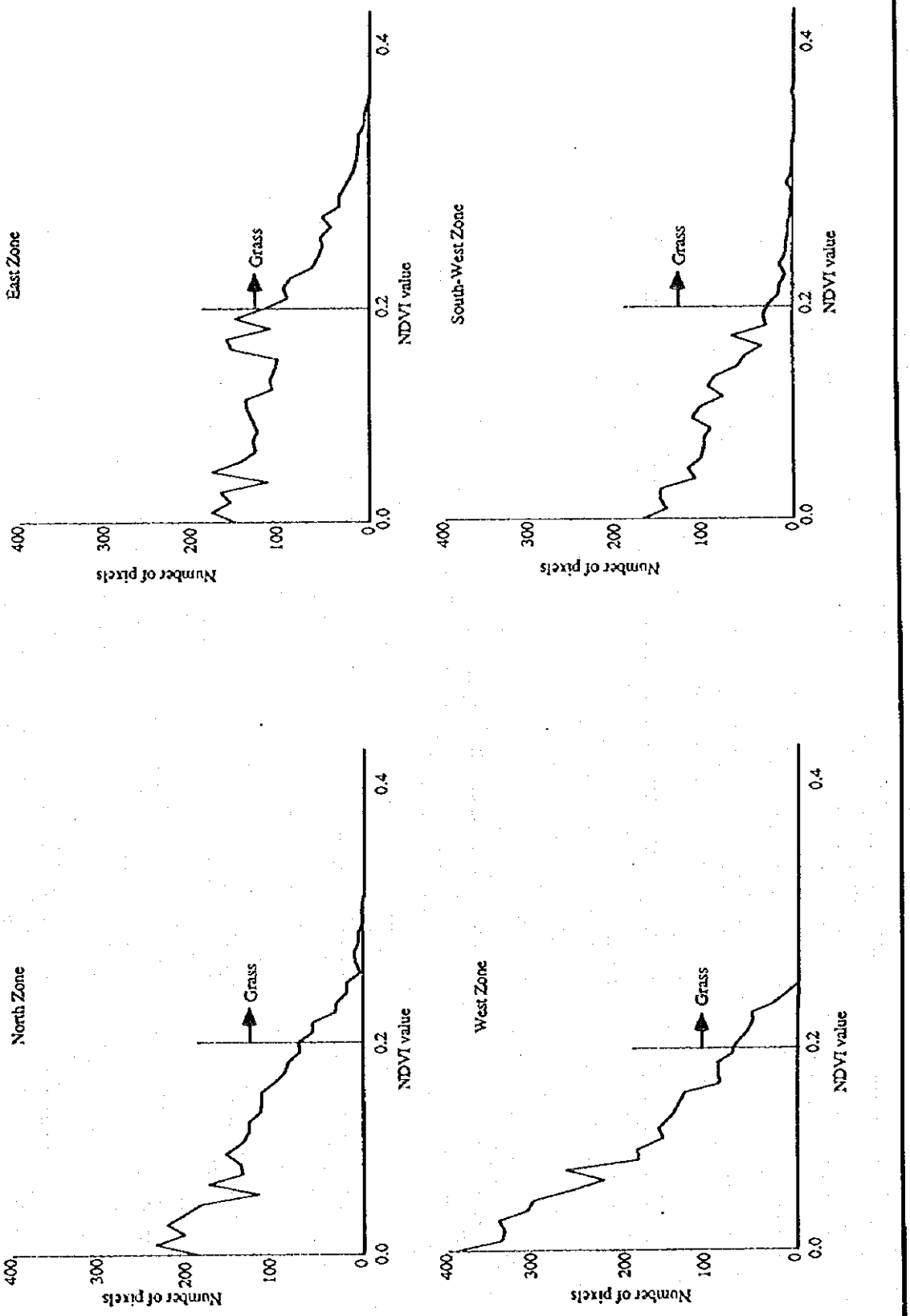

Figure Q.26 Frequency distribution of pixels with increased NDVI for defined zones for the period of 1992 February to 1993 February

THE GOVERNMENT OF THE PHILIPPINES
THE DEPARTMENT OF PUBLIC WORKS AND HIGHWAYS
THE STUDY ON FLOOD AND MUDFLOW CONTROL FOR SACOBIA-BAMBAN/ABACAN RIVER DRAINING FROM MT.PINATUBO
JAPAN INTERNATIONAL COOPERATION AGENCY

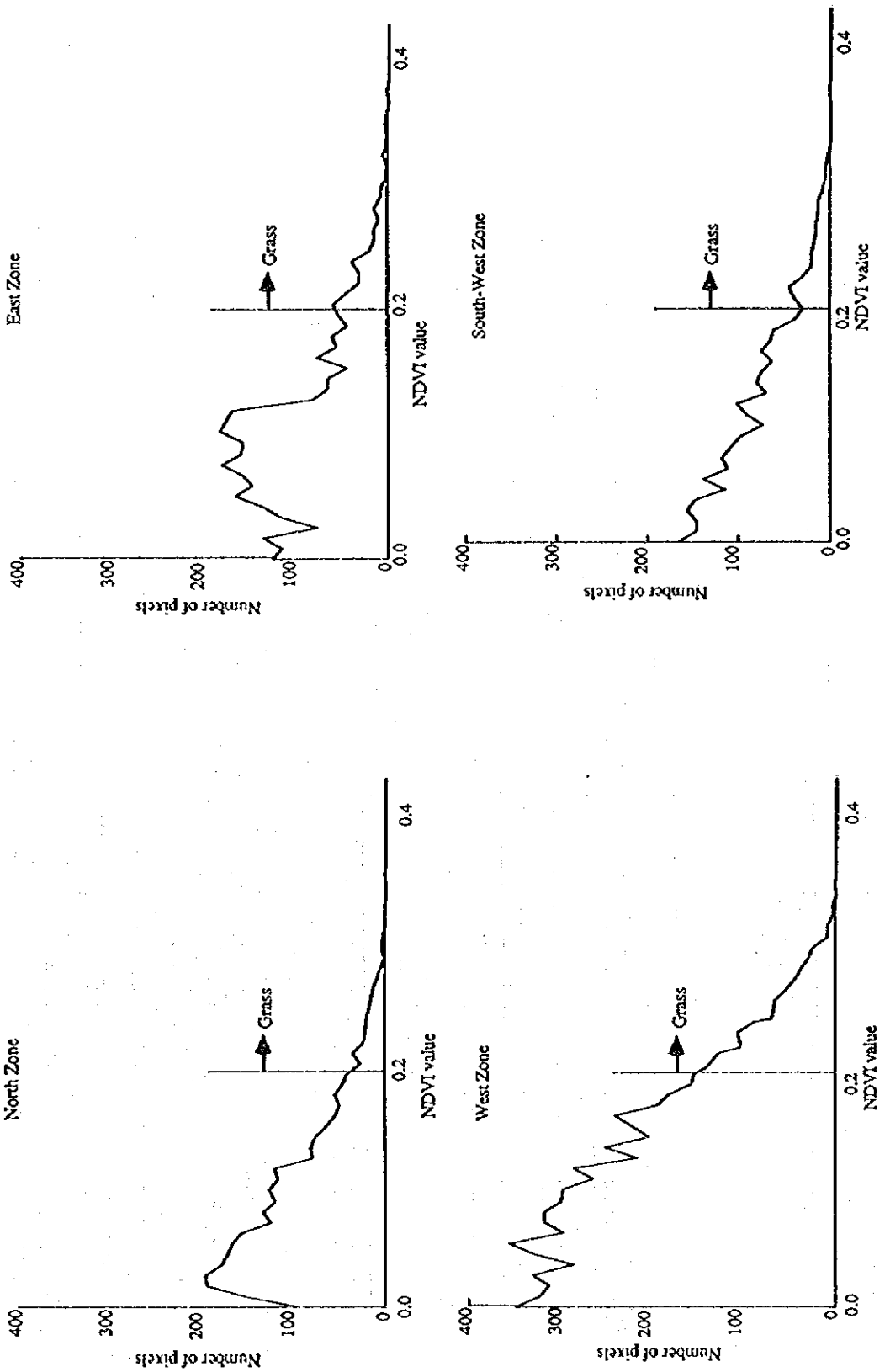

Figure Q.27 Frequency distribution of pixels with increased NDVI for defined zones for the period of 1992 November to 1993 December

THE GOVERNMENT OF THE PHILIPPINES
THE DEPARTMENT OF PUBLIC WORKS AND HIGHWAYS
THE STUDY ON FLOOD AND MUDFLOW CONTROL FOR SACOBIA-BAMBAN/ABACAN RIVER DRAINING FROM MT.PINATUBO
JAPAN INTERNATIONAL COOPERATION AGENCY

APPENDIX R

GIS DATA ANALYSIS

APPENDIX R

GIS DATA ANALYSIS

TABLE OF CONTENTS

Page

CHAPTER 1 INTRODUCTION *R-1*

1.1 Background R-1

1.2 Activities R-1

1.3 Organization of the Report R-1

CHAPTER 2 TRAINING AND TECHNOLOGY TRANSFER *R-2*

2.1 Classroom Training R-2

2.2 On-the-job Training R-2

CHAPTER 3 GIS DATABASE DEVELOPMENT *R-3*

3.1 Aerial Surveys R-3

3.2 Design of the Digital Database R-3

3.2.1 Initial preparation of data R-3

3.2.2 Appending maps for entire region R-4

3.2.3 Preparation of plots R-4

3.3 Preliminary Data Manipulation R-4

3.3.1 TIN models for contour data R-4

3.3.2 Bi color Stereo Images R-5

CHAPTER 4 PYROCLASTIC FLOW ANALYSIS *R-6*

4.1 Procedure for Analysis R-6

4.2 Results of Analysis R-6

4.2.1 Tool for Interactively Specific Deposit Area R-6

4.2.2 Sectional Areas for Flow Deposit R-7

4.2.3 Volume of Flow Deposit R-7

CHAPTER 5 LAHAR DEPOSIT ANALYSIS *R-8*

5.1 Procedure for Analysis R-8

5.2 Results of Analysis R-8

5.2.1 Cross section Development R-8

5.2.2 Sectional Areas for Flow Deposit R-8

5.2.3 Volume of Flow Deposit R-9

CHAPTER 6 MUD FLOW AND FLOOD ANALYSIS *R-10*
6.1 Procedure for Analysis R-10
6.2 Results of Analysis R-10
6.2.1 Maximum Inundation Extent for each Return Period R-10
6.2.2 Inundation Depth Using GIS Modeling R-10

CHAPTER 7 HAZARD ANALYSIS *R-11*
7.1 Procedure for Analysis R-11
7.2 Results of Analysis R-11
7.2.1 Preparation of Asset Information R-11
7.2.2 Value of Assets R-12
7.2.3 Average Annual Damage Value for Floods R-12
7.2.4 Indirect Damage from Traffic Detour R-13
7.2.5 Other Costs R-14

REFERENCES *R-15*

LIST OF TABLES

Table No.	Title	Page
R.1	Schedule of Training Activities	R-16
R.2	List of Data transferred from the MPR-PMO	R-17
R.3	List of Topographic Information in the Digital Database	R-18
R.4	Geomorphological Changes Estimated using GIS Techniques	R-19
R.5	Lahar Deposit along Sacobia-Bamban River Estimated using GIS Techniques	R-20
R.6	Inundation and Mud Flow Area for each Return Period estimated using Simulation and GIS Techniques	R-24
R.7	Value of Assets estimated using GIS Techniques	R-25
R.8	Probable Annual Average Damage from Flood for each Return Period estimated using GIS Techniques	R-26
R.9	Traffic Detour Costs due to Inaccessibility of Bridges estimated using GIS Techniques	R-27
R.10	Evacuation and Clean up Costs from Flood for each Return Period estimated using GIS Techniques	R-28
R.11	Total Affected Population and Land for Maximum Possible Damage in 20 years	R-29

LIST OF FIGURES

Figure No.	Title	Page
R.1	Topographic Information from Aerial Surveys	R-30
R.2	Details of Data Layers in the Digital Database	R-31
R.3	Flow chart for developing plotting Routines	R-36
R.4	Sample Plots used in the Study	R-37
R.5	3-D Stereo Image of the Upper Plains	R-39
R.6	Procedure for Pyroclastic Flow Deposit Analysis	R-42
R.7	Location of Cross Sections for Pyroclastic Flow Deposit Analysis	R-43
R.8	Birds Eye View of Pyroclastic Flow Deposit Area	R-44
R.9	Procedure for Lahar Deposit Analysis	R-45
R.10	Profiles of Cross Sections along Sacobia River	R-46
R.11	Profiles of Cross Sections along Bamban River	R-47
R.12	Procedure for Mud Flow and Flood Analysis	R-48
R.13	Probable Inundation Area for each Return Period	R-49
R.14	Procedure for Flood Hazard Analysis	R-50
R.15	Maximum Flood Hazard Area	R-51
R.16	Probable Damage to Buildings from Flood for each Return Period	R-52
R.17	Probable Damage to Cultivable Land from Flood for each Return Period	R-53
R.18	Probable Damage to Infrastructure from Flood for each Return Period	R-54

CHAPTER 1 INTRODUCTION

1.1 BACKGROUND

The Government of Philippines (GOP) has requested technical assistance from the Government of Japan (GOJ) through the Japan International Cooperation Agency (JICA) to study on flood and mud flow control in the Sacobia-Bamban and Abacan river systems. In accordance with the scope of work for the technical assistance, the JICA Study Team (Study Team here after) has been executing works since November 15, 1993.

1.2 ACTIVITIES

There are two major components in the Geographic Information System (GIS) related activities in the Study. First, a comprehensive program was organized for training and technology transfer on GIS to the DPWH staff. Expatriate and local consultants were assigned through a sub-contract between November 1993 till September 1994 to effectively implement the program and also ensure transfer of digital information between the DPWH and the Study Team. Then, geomorphological analysis, mud flow analysis and hazard analysis were performed using GIS techniques. The GIS expert of the Study Team supervised the training and also performed the analyses using the GIS database.

1.3. ORGANIZATION OF THE REPORT

Chapter 2 discusses the contents of training and technology transfer. Chapter 3 explains the digital database preparation for the study. Chapters 4 through 7 discuss the analyses performed using the GIS database, namely, pyroclastic flow deposit, lahar deposit, flood damage potential estimation and hazard estimation respectively.

CHAPTER 2 TRAINING AND TECHNOLOGY TRANSFER

Under the supervision of the Study Team, comprehensive training was conducted for the DPWH Staff by International consultants through a sub-contract between March 94 and September 94. The terms of reference for the training covers technology transfer, GIS related activities and general technical and operational assistance for the Mt. Pinatubo Rehabilitation Project Management Office (MPR-PMO) of the DPWH. The training was conducted in two phases, Phase I between April - May 94 and Phase II between July - Sep 94. The contract allowed participation by expatriate staff for a total of 6 man-months and local staff for a total of 17 man-months from the consulting group.

2.1 CLASSROOM TRAINING

Training was conducted for 4 PMO staff in approximately 75 hours of lectures, and 100 hours of hands-on practice. The topics for training ranged from map projection, operation of GIS software, CAD software to maintenance of computer systems. A list of the training activities is available in Table R.1. Training in computer hardware and software maintenance involved hands-on experience in basic trouble-shooting activities. Training in software systems development included programming languages and system programming. Certificates of completion of the Training were given away to the trainees in Oct 94.

2.2 ON-THE-JOB TRAINING

At the conclusion of the training in Phase II, a medium-sized GIS project was performed by the trainees. Practical aspects of GIS technology were covered through project activities required for the development of a project database explained in detail in Chapter 3. The MPR-PMO trainees assisted in organizing the existing digital information. All the available digital information in the PMO relevant to the study were transferred to the project database. Additional information on basin boundaries, sabo dams, lahar extent in 1993 and 1994, administrative boundaries were added to the database. A list of the data is available in Table R-2. Several illustrative plots of the study area to a scale 1:50,000 were created by the trainees using the project database. A detailed work report for the contract period was prepared by the subcontractors.

CHAPTER 3 GIS DATABASE DEVELOPMENT

In this study a comprehensive digital database has been developed for the topographic and socioeconomic information. Some existing information in the MPR-PMO were utilized. Several additional information have been created by the Study Team.

3.1 AERIAL SURVEYS

Topographic information were extracted from aerial photographs for three dates 1991, 1992, 1994. The topographic information, namely elevation contours, rivers, roads, houses were extracted to a scale 1:10000 for the study area. The study area is covered by 32 map sheets each with a size 60cm x 60cm.

The data for 1991 is based on aerial photographs of 1:60000, 1:25000 with dates between 1981 and 1991. The data for 1992 is based on aerial surveys of 1:25000 during October 1992. The data for 1994 is based on surveys of 1:15000 done by the Study Team during March 1994. Some areas could not be covered due to lack of information in 1991 and 1992. The main features of the data are shown in Figure R.1.

3.2 DESIGN OF THE DIGITAL DATABASE

A digital database was developed for all the topographic information. The contents of the digital database are given in Table R.3. The digital information was about 300MB before processing. There were 384 layers in the database consisting of 5 categories of information for 3 different years for each of the 32 map sheets. The contents of each data category -- geometry and attributes are described through sample plots in Figure R.2.

3.2.1 Initial preparation of data

The initial preparation includes data organization, classification of contour lines and analysis of the contour data. The study area has been grouped into three areas --the upper river basins, lower plains of Bamban and lower plains of Abacan--for better data handling during analysis. The contour lines were classified to differentiate the contours at every 10m, 20m and 100m for better visibility, using temporary variables that were added to the attribute files of the contour data.

3.2.2 Appending maps for entire region

To perform quick plots and analysis the topographic information for each category were integrated for the entire region from the individual map sheets. The matching of information across the borders of adjacent map sheets was done using GIS techniques. Thus a seamless database for the entire study area was established.

3.2.3 Preparation of plots

After the classification of contour lines, large size (40cm x 200cm) plots were prepared with different combinations, such as contours with roads, contours with rivers, roads, administrative boundaries, lahar disaster area, etc. to scales of 1:20,000 and 1:50,000. The procedure for developing the plots is shown in a schematic diagram (Figure R.3). These plots were used for further reference by working groups. Such maps would not be easily possible with the conventional paper maps, in which only the size can be modified while copying and not the contents. Some other sample plots are also enclosed (Figure R.4).

3.3 PRELIMINARY DATA MANIPULATION

Preliminary data manipulation was required to make the digital elevation data easily utilizable for the analysis. The elevation data was based on different aerial photographs with scales varying from 1:60,000 to 1:15,000 and had varying accuracy of the elevation. Some locations had elevation errors of 10 to 12m. These errors were corrected by experts by comparing the aerial photographs. Thus corresponding locations that were unaffected by the eruption, would have the same elevation in all the 3 years - 1991, 1992, 1994.

3.3.1 TIN models for contour data

The elevation data based on contours for each 5m in the mountain areas and each 2m in the lower plains was modeled in the computer using a Triangulated Irregular Network (TIN) algorithm. The model was input with a weed tolerance of 30m for the contours. Lattices were created with a spatial resolution of 10m from the TINs. The lattices for before eruption (1991), 1992 and 1994 were then further manipulated to develop hillshades, for purpose of presentation.

3.3.2 Bi color Stereo Images

Using special programs, Bi color stereo images were developed to scales of 1:20,000 and 1:160,000, to demonstrate the changes in topography between the before-eruption and after-eruption situations. When viewed with a special lens which has a red film for the left eye and a blue film for the right eye, the bi color stereo image will provide a 3 dimensional effect for the viewers. This technique is much easier and impressive for the views than the conventional way of viewing stereo image pairs. It is particularly useful for mountainous areas where the panoramic effect is not required. The images for before and after eruption for the upper plains, extending from the crator down the slope for about 20km to a scale of 1:160,000 can be seen in Figure R.5. The elevation has been represented at 1:400,000. The development of the crator and the pyroclastic flow deposit can be clearly seen.

CHAPTER 4 PYROCLASTIC FLOW ANALYSIS

The estimation of volume of pyroclastic flow deposit was done using the topographic for two different years, namely, before eruption (1991) and 1992. The data for 1994 was used to estimate the changes after 1992. Originally it was planned to use the pyroclastic flow area estimated by PhiVolcs on 1:50,000 maps and estimate the volume of pyroclastic flow deposit from the changes in elevation (Reference R.1). Then, the pyroclastic flow and mud flow areas estimated by Phivolcs were drawn on 1:50,000 by visual interpretation of aerial photographs. There were also inconsistencies between the maps produced by them in 1992 and 1993 showing the flow delineation.

4.1 PROCEDURE FOR ANALYSIS

It was decided to identify the flow deposit area by the experts in the Study Team and then, estimate the volumes by considering the cross sections at different locations and estimating the changes in elevation in them. Cross sections along North-South were created from the lattices in an automated fashion using GIS techniques. For the pyroclastic flow area, cross sections were created at every 200m from the crator for the crator section (up to 2.4 km from the crator) and at every 500m for the up stream portion (from 2.7 km from the crator till 14.2 km from the crator). The procedure for analysis is shown in Figure R.6.

The cross sections were used in the profile analysis on the lattices for 1991, 1992 and 1994 respectively. The profiling was done with a weed interval of 20m. Profile tables obtained from the analysis contain elevation values along each cross section at every 20m along the length. The location of some typical cross sections is shown in Figure R.7.

4.2 RESULTS OF ANALYSIS

The profile tables for 1991, 1992 and 1994 were matched and joined appropriately so that each record contains the corresponding elevations for all the three years, for any point along a cross section. Using the profile table, graphs were created for presentation and expert interpretation. The pyroclastic deposit area delineated by PhiVolcs was transferred on each cross section, and the extent was included in the graph.

4.2.1 Tool for Interactively Specific Deposit Area

Using mouse, the user can specify the deposit area, by pointing to two locations on the graph, where the section area has to be calculated. The computer will

automatically calculate the section area between the two selected points by summing the spot values and multiplying it by the weed interval. The area selected by the user will be shaded with a specific symbol on the display.

4.2.2 Sectional Areas for Flow Deposit

Using the interactive tool for specifying the deposit area, the pyroclastic flow deposit extent along each cross section was defined. Then, by doing tabular manipulation, the changes in elevation between 1991 and 1992, 1991 and 1994 within the Study Team specified area were estimated for each cross section. Then, the area of deposit for each cross section was estimated. The results are shown in Figure R.7. Bird's eye views of the deposit area as seen from the Clark air base and Watch point No 5 are shown in Figure R.8. The mountain outline before eruption is drawn in the background in the drapes for 1994.

4.2.3 Volume of Flow Deposit

The volume of pyroclastic flow deposit was estimated by summing up the deposit area in each section. The results of the analysis revealed that the volume estimates for the changes between 1991 and 1994 are the most reliable. This volume corresponds to the situation after 3 rainy seasons after eruption. The lahar discharge at every rainy season estimated by the Study Team from reports and surveys were applied to estimate the deposit for other periods. The results were summarized in three portions, namely up stream of Sacobia-Abacan, Pasig and downstream of Sacobia-Abacan. The results are shown in Table R.4.

CHAPTER 5 LAHAR DEPOSIT ANALYSIS

The lahar and mud flow deposit along the Sacobia-Bamban river, between Mactan Gate and San Francisco bridge was estimated by considering the changes in elevation along the cross sections. Ground surveys were conducted at every 600m from the Mactan gate till the San Francisco bridge for measuring the river elevations and river bed width in 1994. The details of these surveys are reported in Appendix F. These results were incorporated in the analysis. The data for 1991 and 1992 was created from the database.

5.1 PROCEDURE FOR ANALYSIS

The cross sections at every 600m were created from the survey lines used in the ground survey. Additional cross sections were created at every 200m between these lines. The lines were located similar to the ground survey lines, that is across the river channel. The lahar area along the down stream of Bamban river, near the sand pockets planned in the JICA study was estimated by Team experts. This was digitally input into the database and used in the analysis. The procedure for analysis is shown in Figure R.9.

5.2 RESULTS OF ANALYSIS

5.2.1 Cross section Development

The cross sections at every 200m were used in the profile analysis on the lattices for 1991, 1992 and 1994. The profiles developed automatically from the GIS database had to be adjusted manually by experts so that the locations which have not changed after eruption are at the same elevation. The differences of about 1 to 2 meters are important in this analysis, although they are unavoidable in the topographic surveys. The ground surveys for river cross section are the most reliable. They were utilized in this correction. The results for some selected cross sections along Bamban River are shown in Figure R.10 and Figure R.11.

5.2.2 Sectional Areas for Flow Deposit

Using the interactive tool for specifying the deposit area, the lahar deposit extent along each cross section was defined. Then, by doing tabular manipulation, the changes in elevation between 1991 and 1992, 1991 and 1994 within the Study Team specified area were estimated for each cross section. Then, the area of deposit for each cross section was estimated.

5.2.3 Volume of Flow Deposit

The volume of lahar deposit was estimated by summing up the deposit area in each section. The results of the analysis revealed that the volume estimates for the changes between 1991 and 1994 are the most reliable. This volume corresponds to the situation after 3 rainy seasons after eruption. The results were summarized in three portions, from the Mactan gate to the Bamban Highway, Bamban River and down stream of San Francisco Bridge. The results are shown in Table R.5.

CHAPTER 6 MUD FLOW AND FLOOD ANALYSIS

Simulation modeling was done for about 20km x 10 km each along the down stream of Bamban and Abacan rivers. The details of the simulation can be seen in Appendix G. The results of numeric simulation modeling consisting of the sediment and inundation depth and extent for floods of return period such as 2, 5, 10, 20, 50 and 100 years were obtained digitally. The data contains the sediment and inundation depth for each 100m x 100m cell, in the simulation area. They were utilized to interpolate inundation maps for the entire study area using GIS techniques.

6.1 PROCEDURE FOR ANALYSIS

The maximum inundation areas for return periods 2 and 100 years were manually created by experts using the results of numeric simulation. It was essential to develop the maximum inundation areas for other return periods. It was also required to extrapolate the flood depth for the areas outside the simulation extent for each return period. The procedure for analysis is shown in Figure R.12.

6.2 RESULTS OF ANALYSIS

6.2.1 Maximum Inundation Extent for each Return Period

The maximum inundation extents for 2 and 100 years were input in the GIS and using a logarithmic area interpolation technique in the GIS, the maximum inundation areas for 5, 10, 20 and 50 years were estimated. The probable inundation area for each return period is shown in Figure R.13.

6.2.2 Inundation Depth Using GIS Modeling

The inundation depth data obtained from simulation and the maximum inundation areas for each return period were modeled using the TIN model in the GIS and new data was created for study area. The data contains the sediment and inundation depth for every 100m x 100m cell. The inundation areas with depth more than 20cm for each return period is summarized in Table R.6.

CHAPTER 7 HAZARD ANALYSIS

The hazard from flood consists of two components namely, the direct damage to buildings, agricultural land and infrastructure, and the indirect damage due to inaccessibility by road. The damage rate is related to the inundation depth and sediment depth at any location.

7.1 PROCEDURE FOR ANALYSIS

The procedure for flood hazard analysis is shown in Figure R.14. The required information for the analysis namely, population in 1994, number of households in 1994, number of establishments in 1994, were obtained based on each barangay. Other land based informations such as the current existing landuse after lahar damage, location of irrigation schemes, roads, buildings and bridges were summarized in terms of corresponding areas in each barangay.

7.2 RESULTS OF ANALYSIS

7.2.1 Preparation of Asset Information

The current landuse for 1990 was updated with the lahar affected area to create the landuse for 1994. Some changes owing to evacuation and resettlement could not be reflected in the extents for built up areas. This map was primarily utilized to estimate the areas of cultivable land for paddy, corn and commercial crops.

(1) Building Information

The location of buildings was available only for about 150 sq. km. along the Bamban river (see Figure R.1). So in order to count the buildings in each barangay in the study area, a linear regression was performed between the building count, and number of house holds and number of establishments. The building information was first summarized as number of buildings in each barangay and this was used in the regression analysis. The following equations were obtained.

No. of residential buildings = 7.7 + 0.85 * No. of households in 1994

($R^2 = 0.70$)

No. of commercial buildings = 4.7 + 0.85 * No. of establishments in 1994

$(R^2 = 0.80)$

These equations were applied to estimate the number of buildings in other barangays.

(2) Irrigation Schemes

The location of each irrigation scheme was input as a point and the scheme was represented by a circle created automatically using GIS techniques around that point corresponding to the size in hectares. The shapes of bigger schemes with areas more than 1000 hectares were digitized manually.

(3) Bridges

The location major bridges were already available in the database. The possible location of other bridges were identified using GIS techniques from the intersection of roads and rivers. An average length and width of 10m and 6m respectively were applied to these bridge for the purpose of analysis.

7.2.2 Value of Assets

The unit cost of maintenance and repair for buildings and infrastructure, and the opportunity costs for loss of productivity of the cultivable land were obtained from Table 10.17 of the main report. The total value of assets were estimated by applying these units to the asset information in the database. The affected area until 1994 was estimated from lahar damaged area identified by PhiVolcs and the Study Team. The value of assets in these areas were discounted to represent the current situation of the assets. The results are summarized in terms of municipalities as shown in Table R.7.

7.2.3 Damage Value for Floods

The inundation areas identified by the mud flow and flood analysis were utilized in the analysis. The maximum flood hazard area is shown in Figure R.15. It represents the situation for the maximum expected flood in 100 years. The

probable areas for other return periods are shown in Figure R.13. The damage rates corresponding to the depth of flood and sediment were obtained from the damage curves in Figure 10.68 of the main report. In this analysis, it was assumed that 100% damage will occur for sediment depths 50cm and 100cm, for buildings and infrastructures respectively.

(1) Calculation of affected assets

The actual damagable value of assets in the affected area was estimated by first calculating the damage rates due to flood and sediment in each 100m x 100m cell in the hazard area. The maximum damage rate, either sediment or flood was selected for each cell. Then the damagable value of assets in each cell was estimated assuming that the assets are uniformly distributed. The damage values were aggregated by each barangay. The analysis was repeated for each type of asset, namely building, land and infrastructure, and each return period. The results are shown in Figures R.16, R.17 and R.18. The results were summarized by each municipality and river basin to estimate the total damagable values for each return period. The results are shown in Table R.8.

7.2.4 Indirect Damage from Traffic Detour

The traffic from Manila, San Fernando and Angeles to Tarlac or Bamban or Concepcion which use either the Bamban or San Francisco bridges will be affected when the bridges become inaccessible. Seven such normal routes were considered in this analysis. They are shown in Figure 10.70 of the main report.

The vehicle operating cost (VOC) of traffic was estimated from the unit cost and the vehicle mix as obtained from other DPWH surveys (see Table R.9). The route detour alternatives when the bridges are not accessible were identified for each of the seven routes. There were totally 15 alternatives consisting of routes for rainy and dry seasons as shown in Table R.9. The traffic diversion length (TDL) was estimated using GIS techniques by calculating the difference between the original and detour routes. The diversion cost (DC) of each detour route was estimated by multiplying the corresponding TDL and VOC. The total diversion cost for each detour was estimated from the average traffic volume, days of detour and DC. The costs were summarized for each normal route. The results are shown in Table R.9.

7.2.5 Other Costs

The costs of evacuation and clean up were estimated for residential buildings separately at rates 4.1% and 1.7% of the damagable value respectively. The results are shown in Table R.10.

The total affected area, land and population for a return period of 20 years was summarized separately as shown in Table R.11.

The area allocated for sand pocket, covering approximately 20 sq. km. can be reclamated and utilized after the completion of various engineering works. The population in this area that will benefit from this reclamation was summarized separately. These are discussed in the main report.

REFERENCES

Ref. No.	Title
R.1	PHIVOLCS, "Mud flow Hazard Map", October 1991.
R.2	Seetharam, K.E., Lal Samarakoon, A. Ishibashi, N. Hirose, *Implementing Very Large Databases using GIS*, Far East Workshop on GIS 93, Singapore.
R.3	Lal Samarakoon, Seetharam, K.E., T. Hashimoto, A. Ishibashi, *"Application of Remote Sensing in Regional Master Plan Development - Integration of GIS Techniques for Land Cover Mapping "* , 15 Asian Conference on Remote Sensing, 1994, India.